

Response to editorial and reviewer Comments for “Simulating Coupled Surface-Subsurface Flows with ParFlow v3.5.0: Capabilities, applications, and ongoing development of an open-source, massively parallel, integrated hydrologic model”

We would like to thank the Executive Editor, the Handling Topical Editor, and the referees for the comments and suggestions intended to improve our manuscript. The minor comments provided by the referees were particularly helpful in bettering specific sections of the manuscript, including some word omissions, typographical errors and clarifications, which can be difficult to spot in one’s own manuscript. The revised manuscript addresses the concerns raised by the referees and we are confident the Editor will find it suitable for publication without an additional external review.

Please find below our revision, which includes detailed point-by-point response to all referee comments. The response to the referee comments are structured as follows: (1) comments from referees, (2) author's response, and (3) author's changes in a marked-up manuscript version showing all the changes made. We are glad to discuss any aspect of the revision with you, the handling topical editor, or any of the referees if questions arise. The original text of the comments is below in plain face font and our responses are given in bold face italic font for maximum clarity. We have included references to specific line numbers regarding all changes and these line numbers refer to the “tracked changes” version to make it as simple as possible to evaluate the changes in the context of the previous submission.

The Executive Editor’s Comments:

This is an executive editor comment highlighting the ways in which this manuscript is not currently compliant with GMD policy on code and data availability. In this case, there is just a single technical issue which needs to be remedied in the revised submission:

1. Github URLs. Github is an excellent development platform, but it lacks the features required of an archive. GitHub themselves tell authors to use Zenodo for this purpose. The authors should follow the procedure detailed there to archive the exact version of the software used to create the results presented: <https://guides.github.com/activities/citable-code/>. The resulting Zenodo repositories present the correct bibliography entries to use. Further details on code and data availability requirements are in the GMD model code and data policy: https://www.geoscientific-model-development.net/about/code_and_data_policy.html. The reasons for the policy and more detail are provided in this editorial: <https://doi.org/10.5194/gmd-12-2215-2019>.

Authors Response

We greatly appreciate the Editor for his comments. The Editor’s directions that we adhere to GMD’s policy on code and data availability and use Zenodo has been considered. We have made modifications to that effect in the revised version of the manuscript. See Lines 985-987 in the revised manuscript.

Anonymous Referee #1 Comments

Authors have summarized major advances in development of an integrated hydrologic

– atmospheric model (ParFlow.*) for simulating terrestrial hydrologic processes. The paper is a nice summary of authors' effort in the past 3 decades on ParFlow development, and its coupling with land surface, atmospheric and reactive transport models. As authors state, the information presented here has been previously published as part of software manuals and papers published by the developers. Therefore, this manuscript provides a valuable resource for the users to learn about the model functionality

However, it would be more useful if authors consider adding the following information:

1. The paper falls short in describing capabilities of ParFlow in comparison to other integrated hydrologic models such as CATHY, HydroGeosphere, etc. This will help users with model selection for a particular application.

Authors Response

We agree with the reviewer that it is important to understand how one integrated model compares to others but note that this has been done recently. The integrated model inter-comparison project was a series of workshops where the developers of many of the contemporary integrated models got together and designed test cases for comparison. Some of these results are highlighted in Maxwell et al. 2014, Kollet et al. 2017 and Koch et al. 2016. Given the extensive work presented in these existing papers, and the extraordinary effort it takes to run such simulations, we feel that including a detailed comparison here is beyond the scope of the review, but we have emphasized these inter-comparison resources for the readers.

2. It would be very useful if authors could describe future model development. What is next?

Authors Response

Absolutely, and we are glad to add these details. We had mentioned the availability of a software development and sustainability plan to improve the capabilities of ParFlow in the last paragraph of the manuscript, but details on future directions were an unintended omission in the draft. We have added text concerning the code developers next plan in improving the code such as new formulations of both kinematic and diffusive wave approximations, and advanced parallelization support (GPU'S and heterogeneous compute architectures) (Lines 968-970). We also note that the development branches and forks can be viewed on the GitHub page (<https://github.com/parflow>).

3. Despite improved parallel efficiency for large scale application, model application for large domains is computationally intensive. Can authors provide further guidelines for model set-up (table of inputs), initialization and calibration? Are there any efforts underway to improve computational time?

Authors Response

We completely agree with the sentiment of this comment; 3d Richard's equation and overland flow is computationally expensive and even the best parallelism cannot change that

fact. One of the challenges to providing guidance here is that ultimately it is up to the user to determine what level of complexity is appropriate for their problems and what portions of the problem to simplify. That level of complexity combined with the heterogeneity of specific elements dictates how long it takes the model to iterate, which is the main factor during initialization and also for calibration. The long run times often inhibit or prevent calibration efforts, so many integrated models to date have not been calibrated and instead are used as virtual hypothesis testing platforms; we're not saying this is necessarily a "best practice in modeling" (we think sensitivity analysis and uncertainty quantification should always be included in planning models) but uncalibrated models that are based directly on the physics can still provide useful results about process interactions. As for initialization, the common practice is to "spin-up" (e.g. Seck et al. 2015) the model to a steady- or pseudo-steady (in the case of a transient forcing) state, but even for one specific kind of model there are multiple workflows that can be used, so this could not be one table rather a tangled spider web. We absolutely agree that guidance is useful in these areas but respectfully disagree that an overview of a particular model is the best place for such guidance. However, recognizing the importance of this comment, we have added clarifying text noting that the studies involving ParFlow outlined in Table 1 provide a wealth of knowledge regarding domain setup (Lines 536-543). Since these are all specific applications, their information will likely be very useful to modelers trying to build a new domain for a similar application as they are setting up and planning their model. As for efforts to improve efficiency, the numerical solvers developed for ParFlow now comprise the core of the Hypre and Sundials solver libraries (the common PFMG preconditioner in Hypre stands for ParFlow Multi-Grid) and are currently the most numerically efficient solvers available. As such, many ParFlow developers are currently focused on increasing performance on heterogenous compute architectures, as noted above in our response to comment 2.

4. While authors summarized various application of the model in Table 2, it would be great if they can present a simple case study that compares computational time as different components are added from land surface to the atmosphere, and show how simulated outputs have been improved compared to observations.

Authors Response

We are in complete agreement that this is common question and that it would be great to have such a table, but in practice it is extremely difficult to provide any general examples like this because of the nonlinearities in the different parts of the solution of the system. For example, the geochemical systems in ParCrunchFlow compared to the nonlinear snowmelt processes in CLM, or the switching on or off of the overland flow routing. Each of these has a different cost, and when coupled to other portions of the problem the numerical cost (i.e. solver time) of their interactions is, for all intents and purposes, impossible to generalize. The best one could do is to highlight a few specific, contrived examples that could never be considered generalizable. The best estimate of how solver time changes would be considering the number of floating-point operations per iteration, but even this cannot be predicted

because the nonlinear system evolves over time so the number of iterations for convergence constantly changes. The relevance of this comment is without question, but it is also deceptively difficult to resolve. Many of the studies presented in Table 1 include computational times for problems with different complexities where ParFlow was used, and this may be able to help readers infer how runtime will change; we have added comments to this affect (Lines 518-527). If one could predict how adding processes would affect runtime that would be an incredible advance for scientific research, but we are aware of no such advances. The best we can offer the reader is a brief summary of these thoughts and their justification (Lines 518-527), which we think the reviewer will agree will be a useful discussion for the readers

Minor Comments

Lines 82-85- The differences between the integrated approach and indirect approach is not clear. Please explain.

Authors Response

This is a good point. After reviewing the original text, we completely agree that this was not clear, and have modified to accommodate suggestions. For example, further descriptions on how ParFlow employ these approaches pertaining simulation of flows in surface and subsurface domains (Lines 87-91) of the revised manuscript.

Line 94 – Kollet et al. (2010) does not seem to be a suitable reference here as the focus of the paper is on parallel efficiency. Please refer to Kollet and Maxwell (2008), Water Resources Research instead.

Authors Response

We absolutely agree; clearly, the citations were mixed up. This has been corrected (Line 100 in the revised manuscript) and we're grateful for the reviewer's sharp eyes.

Line 139 – Is the variable vertical discretization only possible with the terrain following grid option in ParFlow?

Authors Response

Variable vertical discretization can be used with any domain/grid; however, it usually makes the most sense to do so with a terrain following grid since this is commonly used to increase the resolution of the shallow soil layers (Lines 150-151 in the revised manuscript).

Line 155 – Remove “of” from “relative of saturation”

Correction made See Line 168 in the revised manuscript.

Line 171- According to equation 4, units of Darcy flux should be LT⁻¹.

Authors Response

A rather embarrassing mistake on our part that has been corrected. See Line 170 in the revised manuscript.

Section 2.3. Add information regarding flow routing approach. For example, does the new version support D8 flow direction?

Authors Response

D4 flow direction is implemented in ParFlow. Notes have been added to explain this (Lines 220-222).

Line 194 – Move “slope” before the “(gravity forcing term)”

Authors Response

Change made. See Line 211 in the revised manuscript.

Line 254 – Add “relative” to Si

Authors Response

“Relative” has been added. See Line 275 in the revised manuscript.

Line 742- To main consistency, write units.

Authors Response

The units are now provided for all variables presented. See Lines 798-800 in the revised manuscript.

Anonymous Referee #2 Comments

The motivation (and objective) of the paper is stated as (Lines 71-74) : “The purpose of this manuscript is to provide a current review of the functions, capabilities, and ongoing development of one of the open-source integrated models, ParFlow, in a format that is more accessible to a broad audience than a user manual or articles detailing specific applications of the model”. I am very familiar with integrated hydrologic models, but not with ParFlow, and I therefore belong to the target audience. However, after very carefully reading the paper (some sections more than once because they could be clearer), I conclude that the paper does not reach its objective and does not provide a clear review of the code’s functions, capabilities, and ongoing development.

Overall, the organization and writing should be improved to make the text much clearer. Some sections provide too much information on peripheral details and too little on some important points. That is especially the case for the coupling section (section 5), which does not provide a clear picture of the code’s capabilities with respect to its coupling with other codes.

I provide below more detailed comments on specific sections of the paper.

Title

The title is not representative of the content of the paper.

- With respect to coupling, a good portion of the paper focuses on describing the coupling of ParFlow with other codes. The focus is therefore not so much on coupled surface and subsurface flow as the title suggests. Actually, the surface and subsurface coupling could be described more clearly (see comment below).
- The capabilities are described but the paper does not provide a clear picture of the applicability limits of the model.
- The ongoing development is not really addressed. The paper rather lists past developments

Authors Response

The reviewer’s statement that “The title is not representative of the content of the paper” is to some extent a reasonable criticism and appears to be constructive in nature. However, we are faced with a choice and must decide amongst many possible tradeoffs. While it has been coupled to many different codes, the main function of ParFlow is to simulate coupled overland (surface) and subsurface flows, which is reflected by the title. We concede that a different title might be able to capture the complex nature of all the possible simulations but stop short of changing to a complete list of all the couplings included. However, to address these concerns, we have clarified the content and scope in the abstract (Lines 35-38).

We think the applicability of ParFlow has been well discussed in section 6 (Discussion and Summary) highlighting challenging hydrologic projects or research works where ParFlow was used. For example, the code has been applied to simulate surface and subsurface flows at varying spatial scales i.e. from mouth of continental river basins at high resolutions, evaluate relationship between topography and groundwater flow, assess resilience of water resources and anthropogenic stressors, and simulate atmospheric, surface and subsurface energy and water budgets in coupling with other models. . The impetus is on the individual modeler to select a model that is applicable to their task, and we think the paper presents sufficient example for readers to inform their own opinions on when the approach is applicable.

To the final point, we completely agree that we should have included these details before and thank the reviewer for catching this omission. The manuscript has been revised to add ongoing development plan in the last paragraph such as incorporation of new formulations of both kinematic and diffusive wave approximations, and advanced parallelization support (GPU’S and heterogeneous compute architectures). Lines 968-970 in the revised manuscript.

Introduction

The introduction does not fit with the purpose of the paper, which is to present an overview of ParFlow’s capabilities.

- There are some very broad statements on integrated hydrologic models (IHMs) in the first paragraph that are not really required since the intended audience will likely be already aware of IHMs and will not need to be convinced of their usefulness.

Authors Response

We thank reviewer for this critical evaluation, and think we understand their intent, but we disagree that the general statements on integrated hydrologic models (IHMs) are superfluous. Our intended audience is not only those well-vested or with broad knowledge in numerical or hydrologic modeling but include those looking to learn more about IHMs (e.g. graduate students) of whom we hope will consider ParFlow. We believe it would be useful to such potential code users and readers to know what IHMs are in broad strokes, what they do and why ParFlow belongs to that class of simulation platforms.

- The second paragraph (lines 75-94) provides a short summary of ParFlow's surface and subsurface flow capabilities. It is somewhat confusing to provide this summary in the introduction since the main goal of the paper is to provide a much broader overview of the code.

Authors Response

We think this is a good point. The intent was not to summarize coupled surface-subsurface flow simulation in the introduction section but provide introductory statements of such capability of ParFlow and then explain further in section 2 of the paper, which we did in sections 2.1, 2.2, and 2.3. Further, a brief introduction needed to be provided to lead our readers to what is to be discussed in the paper in terms of surface-subsurface flow simulation by ParFlow.

- Lines 95-103 provide a list of previous studies but the description of the scale of application is confusing (large domains, small catchments, complex terrain, large watersheds, continental scale...). Also, the main conclusions or results of these studies are not mentioned. Just citing papers is not helpful. It would be better to comment on these studies to provide the reader with a clearer understanding of the code's applicability. There are several other instances where a list of ParFlow applications is given, without much detail, (example are lines 132-139, lines 161-163, lines 870-875), which generates repetition.

Authors Response

It is completely true that scale can be arbitrary; this is an appropriate criticism and we concur with the reviewer. The manuscript has been revised according to the reviewer suggestion to give numerical evidences to the use of description of the scale of application such as large domains, small catchments, and large watersheds. This is fully exemplified in Table 2 where all of these descriptions are given values of lateral and vertical extents based on the referenced studies (Lines 103-107 and 111-113 in the revised manuscript).

- Section 1.1 on the development history is interesting and relevant (although lines 132-139 can be removed).

Authors Response

We thank the reviewer for this suggestion, however, we'd be glad if this is reconsidered, because Section 1.1 gives a general trajectory of the code's development based on periodic modifications and applications that assesses the code's capabilities. Lines 132-139 (in the original manuscript) end the section with brief recount of some of the recent tested additional modifications and applications which were discussed in subsequent sections of the manuscript. So, we view the presentation in those lines very necessary in the manuscript.

Core functionality

- It is not clear why variably-saturated and steady-state saturated modes are identified separately. Equation 1 is the transient variably-saturated flow equation and equation 3 is derived from the same equation by setting the time derivative to zero and both relative permeability and saturation 1.0. Why treat them separately, especially since a common solution method is used (line 148)? I would only present equation 1 to avoid confusion.

Authors Response

The two equations (1 and 3) were presented to elaborate the fact that the steady-state saturated flow can be derived from the variably saturated flow. This was done for the purpose of simplification and clarity of the equations, but we agree that additional clarification is needed here. However, ParFlow does include a direct solution option for the steady-state saturated problem that is distinct from the transient solver and this note has been added (Lines 188-191).

- Lines 179-185 are out of place and probably not necessary. If they are kept, they should go into an introduction. Same comment for lines 293-300.

Authors Response

The reviewer finds lines 179-185 and 293-300 (in the original manuscript) unnecessary and out of place, but we wish he takes a second look into that. We found it highly essential to begin each section or subsection with a brief introduction or background to lead our readers into what is it we'd be discussing in the said section of the manuscript. Moreover, large portion of the information provided in those lines (in the original manuscript) have been presented differently to some extent in the introduction section of the manuscript (Lines 51-59 revised manuscript). Lines 196-204 only elaborate notes introduced in section 1 of the manuscript.

- The description of the coupling between surface and subsurface (pages 8-9) is confusing and should be clarified. I think that there is two-way coupling in ParFlow but the text suggests that there is only flow from surface to subsurface (see lines 204-206: "To account for vertical flow (into the subsurface from the surface), a formulation that couples the system of equations through a boundary condition at the land surface becomes necessary"). Figure 1 suggests the same one-way flow direction.

Authors Response

This was poorly phrased on our part. There is a two-way coupling of the surface and subsurface flows in ParFlow and we have revised to make that clear (Lines 225; and 233-234).

- It is also not clear if surface and subsurface are coupled everywhere during a simulation or only at limited locations. Section 3.4, which describes the solution for the coupled surface and subsurface flow system, seems to suggest that surface flow is not solved everywhere (although I am not entirely sure because section 3.4 would have to be written more clearly).

Authors Response

Surface-subsurface coupling can occur anywhere in the domain during a simulation and it can change dynamically during the simulation. Coupling between subsurface and surface or overland flow in ParFlow is activated by specifying an overland boundary condition at the top surface of the computational domain, but this mode of coupling allows for activation and deactivation of the overland boundary condition during simulations where ponding or drying occur. Overland flow may occur by the Dunne or Horton mechanism depending on local dynamics. Overland flow routing (kinematic or diffusive wave) is enabled when the subsurface cells are fully saturated. Clarifications of these points have been made on Lines 464-471 in the revised manuscript.

- I do not see the usefulness of section 2.4. There is no evidence that the multiphase flow capabilities are used and the explicit time-weighting scheme used for transport is extremely restrictive for real applications, as well as the absence of dispersion or diffusion. It seems like these options are seldom used.

Authors Response

We agree with the reviewer to some extent, that the multiphase flow capabilities of ParFlow have had limited applications in recent times. However, we provided this functionality of the code to prompt or alert potential code users of the existence of that verified and working capability of ParFlow.

Equation discretization and solvers

- The writing style is clearer for this section, compared to the rest of the paper, but there are still some inconsistencies. For example, the method used to solve the variably-saturated flow equation is mentioned in 3 different places, but it is not consistent
- Lines 365-367: for variably saturated subsurface flow, ParFlow does this with the inexact Newton-Krylov method implemented in the KINSOL package
- Lines 372-373: For variably saturated subsurface flow, ParFlow uses the GMRES Krylov method
- Lines 409-410: For variably saturated subsurface flow, ParFlow uses the Newton-Krylov method coupled with a multigrid preconditioner

Authors Response

The different solvers mentioned in Lines 386-387 are all existing options in ParFlow capable of solving variably saturated subsurface flow equation. Inexact Newton is consistent across all but the preconditioners can be manually changed. The choice of a solver depends on the specific problem(s) being solved, and the code user may select which solver to use. For example, for a particular problem, one solver may provide faster convergence compared to the other. In that case, that solver may be the choice of the code user.

- Similarly, for saturated flow, it is written
- Lines 415-416: For saturated flow, ParFlow uses the conjugate gradient method also coupled with a multigrid method
- Lines 430-431: ParFlow uses the multigrid-preconditioned conjugate gradient (CG) solver to solve the groundwater equations under steady-state, and fully saturated flow conditions
- Either the conjugate gradient method coupled with a multigrid method and the multigrid-preconditioned conjugate gradient represent the same solution method (in which case there is unnecessary repetition) or they are different solution methods (in which case some more information is required).

Authors Response

Conjugate gradient method coupled with multigrid method and the multigrid-preconditioned conjugate gradient for saturated flow are different ways of presenting the solver in the performance of its function and not necessarily repetition.

Coupling

Section 5 on coupling is the section that requires the most careful revision.

- PF.CLM: It is mentioned that a modified version of CLM was incorporated into ParFlow. There is no clear description of the modified CLM (only some examples of capabilities, as listed starting on line 552). There is also no mention of the differences between the modified CLM and the original CLM published by Dai et al. (2003). Considering the aim of the paper, it would be useful to at least list the main capabilities and types of applications, instead of referring to previous work (lines 566-567). There is a mention of comparison to uncoupled models (line 588) but no identification of what the uncoupled models are. Also, since the modified CLM has been integrated into ParFlow, PF.CLM is not really a coupled model in the same sense as the other coupled models presented in section 5.

Authors Response

The difference in module structure between the original CLM and the modified version integrated into ParFlow was provided in the original manuscript. See Lines 620-631 of the revised manuscript.

It may not be feasible to enlist all the capabilities and application of ParFlow presented in the previous research works in details. We believe highlighting essential capabilities and /or applications such as the capability of PF.CLM to predict accurately root-depth soil moisture and referring readers and

potential code users to those resources where tested and specific applications are provided in detail would be useful.

The phrase “uncoupled model” simply meant a stand-alone model used in a simulation e.g. performing a simulation with CLM (land surface model) to compute soil moisture content without coupling with other model (ParFlow), then CLM is an uncoupled model in that regard. We have explained this in the revised version of the manuscript in Line 643.

- ParFlowE.CLM : The section mentions that a 3D heat transport equation has been added to ParFlow, which becomes ParFlowE. Since heat transport appears to be a core feature, why is it only mentioned here instead of being presented much earlier in Section 2? Is it because ParFlowE is a different ParFlow? Also, it is really not clear if the CLM used in ParFlowE.CLM is the same as in PF.CLM. Is ParFlowE available to use with the other models listed in Section 5?

Authors Response

ParFlowE was not included to section 2 because it is a modification made to ParFlow for a specific application. It is included in section 5 because ParFlowE is essentially ParFlow with 3D heat transport formulation addition and coupled to the CLM. It was explicit in the manuscript the original CLM by Dai et al., 2003 was used in coupling ParFlowE.

- ParCrunchFlow: That section is confusing. There is a description of CrunchFlow and its solution methods (lines 769-794) but it looks like only the reaction terms computed by CrunchFlow are used by ParFlow and the advective-dispersive transport capabilities are not used. If that’s the case, I would not describe all the CrunchFlow features, only those used. It would also be interesting to indicate why CrunchFlow’s advective-dispersive transport capabilities are not used and the advection-only capability of ParFlow is used instead, with its restrictive explicit time-weighting scheme. I assume that it’s a question of dimensionality but it is not clearly stated. Also, the reader has to guess that ParCrunchFlow is only applicable for subsurface simulations (it should be clearly stated). The whole section would need to be rewritten more clearly.

Authors Response

The document has been revised to highlight why CrunchFlow’s advective-dispersive transport capabilities are not used in the coupled model (ParCrunchFlow). ParCrunchFlow makes use of multidimensional advection capability of ParFlow instead of CrunchFlow’s advective-dispersive transport capabilities (up to two-dimensional). See Lines 861-863 in the revised manuscript. It been made in the revised manuscript that ParCrunchFlow is applicable only in the subsurface. See Line 852 in the revised manuscript.

- The terminology used to describe the coupling of ParFlow with other codes is not consistent and can be confusing. There is a mention of offline and online couplings in section 5, which are fairly clearly described, but those terms are not used after that. It would be clearer if a constant terminology was used to describe the type of coupling.

Authors Response

The entire section 5 has been revised for consistency in the use of terminologies “online” and “offline” couplings. See Lines 635, 689, 736, 807, and 859

Discussion and Summary

That section does not contribute much to the paper. Some sentences and statements are too general. One example is the first paragraph of the section.

The very last paragraph provides some practical information about ParFlow. From the point of view of a potential user or developer, it would be interesting to develop that aspect. For example, there is a mention that a software development and sustainability plan exists. It would be very interesting to provide a summary of that plan. Also, community models have their challenges. For example, how is the model verified once modifications have been made? Is there a series of verification examples? Is there a single version or have many “branches” been developed over the years? If there are many branches or versions, how are they managed? Who is responsible for maintaining the code and designing the development and sustainability plan? What are the main issues faced by a user (new or experienced)?

Authors Response

We have included further descriptions to the software development and sustainability plan for ParFlow such as new formulations of both kinematic and diffusive wave approximations, and advanced parallelization support (GPU'S and heterogeneous compute architectures). See Lines 967-969 in the revised manuscript.

Sources to all versions and/or releases of the code has been provided in the “code availability and data policy” section where code developers and contributors can be found. This is not included in the main text to prevent redundancy. See Lines 984-986 in the revised manuscript.

ParFlow’s maintenance and development and sustainability plans are designed by group of code developers and scientists from various institutions listed in Lines 131-135 in the revised manuscript.

Lastly, ParFlow has a clear, rigorous verification procedure to make sure that any changes checked in do not “break” previous developments. This ensures numerical accuracy and backwards compatibility. The full suite of test cases is automatically re-run before any submitted change can even be considered for merging with the master branch of the code. The number of branches/forks cannot be controlled in any open source (or community) code, but any contributions to the master branch are exhaustively vetted before being pushed out to users. A note explaining this procedure has been added (Lines 958-969).

Tables and Figures

Table 2 provides an overview of coupling studies but with very little information and one has to refer to the individual publications to have a better understanding of these simulations (and ParFlow’s capabilities). In that table,

- The simulation scale is not clear since there are mentions of watershed and catchment but it is not clear what size they are. There is also a mention of regional scale but no indication on how it is different from catchment or watershed. I suggest that some information on the size of the model (for example the area and perhaps the depth) be given.

Authors Response

Table 2 has been revised to define the sizes (i.e. lateral and vertical dimensions) of catchment, watershed, regional scale as used in the original articles mentioned in the manuscript (Lines 1125-1127).

- It would be informative, for a potential user, to indicate which studies are conceptual (e.g. model development, numerical methods) and which are application to real systems, with a mention if there was a model calibration to observations.

Authors Response

Table 2 has been revised to indicate whether the original study was model development and if there was a model calibration to observations.

Figure 7 is not referenced in the text.

Authors Response

The paper has been revised to reference Figure 7 in the text. See Line 902 in the revised manuscript.

Symbols and equations

The symbols used in the equations have to be checked for consistency. There are several instances where the same letter or symbol designates different quantities and cases where the same quantity is identified with a different symbol (one example is hydraulic conductivity). Also, some variables (one example is porosity) are defined more than once. I am not providing an exhaustive list but some examples are:

- Equation 2: x is not defined

Authors Response

Equation 2 has been revised to define all variables appropriately (Line 167).

- In equation 2, p is pressure head but it is hydraulic head in equation 4

Authors Response

The symbols for pressure head and hydraulic head in Equations 2 and 4 have been revised. Different symbols have been used (Lines 167 and 186).

- Units for q_s in equation 1 are given as L^3T^{-1} , which is not consistent with the units for equation 1.
- q_s is used in both equations 1 and 5 but it is not the same quantity since the units are different in the two equations.

Authors Response

The units of q_s in Equations 1 and 5 have been revised to be equal (Line 172 and 207).

- Equation 5 could be deleted and replaced by equation 9

Authors Response

Equation 5 is a lead to equation 9 so we believe it does not make it less important including it.

- Equations presented in section 5 should be carefully reviewed because they have obviously been copied from other documents and have not been checked for consistency with respect to the ParFlow equations presented in section 2.

Authors Response

Equations in section 5 have been revised for consistency in the equations where appropriate.

Anonymous Referee #2 Comment

Writing

Careful proofreading is required because there are several instances where words are missing or where a sentence or expression is not clear. I am not providing an exhaustive list but some illustrative examples in the beginning of the paper are:

- Line 57: “vadose flow”. Should be something like vadose zone flow.

Authors Response

Line 57 is revised to include “zone” to vadose flow. See Line 57 in the revised manuscript.

- Lines 58-59: “process domains”. Not sure what process domains are.

Authors Response

Lines 58-59 have been revised. See Line 59 in the revised manuscript.

- Lines 62-63: “hydraulically-linked interconnected” is redundant

Authors Response

Text in Line 63 are revised to eliminate redundancy. The phrase “hydraulically-connected” is used.

- Line 64: “feedback between the components”. Components is not defined and it is not clear what it refers to.

Authors Response

Components represented surface and subsurface flow systems, and the text has been revised as such in Line 64.

- Lines 75-76: “surface, unsaturated, and groundwater flow”. There should not be any distinction between unsaturated flow and groundwater flow. Flow in the unsaturated zone is groundwater flow.

Authors Response

“Unsaturated” has been removed. See Line 76 in the revised manuscript.

- Line 77: “surface and overland flow”. Is surface flow different from overland flow? The paper uses both terms without specifying if they are synonyms or represent different flow processes (which this sentence is suggesting). The paper should be checked for consistency in using surface and/or overland flow.

Authors Response

The paper is revised to use surface or overland flow as synonyms.

1
2 **Simulating Coupled Surface-Subsurface Flows with ParFlow v3.5.0: Capabilities,**
3 **applications, and ongoing development of an open-source, massively parallel, integrated**
4 **hydrologic model**

5
6
7
8 Benjamin N. O. Kuffour^{1,*}, Nicholas B. Engdahl¹, Carol S. Woodward²,
9 Laura E. Condon³, Stefan Kollet^{4,5}, and Reed M. Maxwell⁶

10
11
12 ¹Civil and Environmental Engineering, Washington State University, Pullman, WA, USA

13 ²Center for Applied Scientific Computing, Lawrence Livermore National Laboratory, Livermore,
14 CA, USA

15 ³Hydrology and Atmospheric Sciences, University of Arizona, Tucson, AZ, USA

16 ⁴Institute for Bio- and Geosciences, Agrosphere (IBG-3), Research Centre Jülich, Geoverbund
17 ABC/J, Jülich

18 ⁵Centre for High-Performance Scientific Computing in Terrestrial Systems, Geoverbund ABC/J,
19 Jülich

20 ⁶Integrated GroundWater Modeling Center and Department of Geology and Geological
21 Engineering, Colorado School of Mines, Golden, CO, USA

22
23 *Correspondence to:* Benjamin N. O. Kuffour (b.kuffour@wsu.edu)

27
28
29
30
31
32
33
34
35
36
37
38
39
40
41
42
43
44
45
46
47
48

Abstract

Surface and subsurface flow constitute a naturally linked hydrologic continuum that has not traditionally been simulated in an integrated fashion. Recognizing the interactions between these systems has encouraged the development of integrated hydrologic models (IHMs) capable of treating surface and subsurface systems as a single integrated resource. IHMs is dynamically evolving with improvement in technology and the extent of their current capabilities are often only known to the developers and not general users. This article provides an overview of the core functionality, capability, applications, and ongoing development of one open-source IHM, ParFlow. ParFlow is a parallel, integrated, hydrologic model that simulates surface and subsurface flows. ParFlow solves Richards' equation for three-dimensional variably saturated groundwater flow and the two-dimensional kinematic wave approximation of the shallow water equations for overland flow. The model employs a conservative centered finite difference scheme and a conservative finite volume method for subsurface flow and transport, respectively. ParFlow uses multigrid preconditioned Krylov and Newton-Krylov methods to solve the linear and nonlinear systems within each time step of the flow simulations. The code has demonstrated very efficient parallel solution capabilities. ParFlow has been coupled to geochemical reaction, land surface (e.g. Common Land Model), and atmospheric models to study the interactions among the subsurface, land surface, and the atmosphere systems across different spatial scales. This overview focuses on the current capabilities of the code, the core simulation engine, and the primary couplings of the subsurface model to other codes, taking a high-level perspective.

49 1. Introduction

50 Surface and subsurface (unsaturated and saturated zones) water are connected components of
51 a hydrologic continuum (Kumar et al., 2009) . The recognition that flow systems (i.e. surface and
52 subsurface) are a single integrated resource has stimulated the development of integrated
53 hydrologic models (IHMs), which include codes like ParFlow (Ashby and Falgout, 1996; Kollet
54 and Maxwell, 2006) , HydroGeoSphere (Therrien and Sudicky, 1996), PIHM (Kumar, 2009), and
55 CATHY (Camporese et al., 2010) . These codes explicitly simulate different hydrological
56 processes such as feedbacks between processes that affect the timing and rates of
57 evapotranspiration, vadose zone flow, surface runoff and groundwater interactions. That is, IHMs
58 are designed specifically to include the interactions between traditionally incompatible ~~process~~
59 flow domains (e.g. groundwater and land surface flow) (Engdahl and Maxwell, 2015) . Most IHMs
60 adopt a similar, physically-based approach to describe watershed dynamics where the governing
61 equations of three-dimensional variably saturated subsurface flow are coupled to shallow water
62 equations for surface runoff. The advantage of the coupled approach is that it allows hydraulically-
63 ~~linked-interconnected~~connected groundwater-surface water systems to evolve dynamically, and
64 for natural feedbacks between the ~~components-systems~~ to develop (Sulis et al., 2010; Maxwell et
65 al., 2011; Weill et al., 2011; Williams and Maxwell, 2011; Simmer et al., 2015). A large body of
66 literature now exists presenting applications of the various IHMs to solve hydrologic questions.
67 Each model has its own technical documentation, but the individual development, maintenance,
68 and sustainability efforts differ between tools. Some IHMs represent commercial investments and

69 others are community, open-sourced projects, but all are dynamically evolving as technology
70 improves and new features are added. Consequently, it can be difficult to answer the question of
71 “what exactly can this IHM do today” without navigating dense user documentation. The purpose
72 of this manuscript is to provide a current review of the functions, capabilities, and ongoing
73 development of one of the open-source integrated models, ParFlow, in a format that is more
74 accessible to a broad audience than a user manual or articles detailing specific applications of the
75 model.

76 ParFlow is a parallel integrated hydrologic model that simulates surface, ~~unsaturated,~~ and
77 groundwater flow (Maxwell et al., 2016). ParFlow computes fluxes through the subsurface, as well
78 as interactions with above-ground or surface ~~and (overland)~~ flow: all driven by gradients in
79 hydraulic head. Richards’ equation is employed to simulate variably saturated three-dimensional
80 groundwater flow (Richards, 1931). Overland flow can be generated by saturation or infiltration
81 excess using a free ~~surface~~ overland flow boundary condition combined with Manning’s equation
82 and the kinematic wave formulations of the dynamic wave equation (Kollet and Maxwell, 2006).
83 ParFlow solves these governing equations employing either a fully coupled or integrated approach
84 where surface and subsurface flows are solved simultaneously the Richards’ equation in three-
85 dimensional form (Gilbert and Maxwell, 2016) , or an indirect approach where the different
86 components can be partitioned and flows in only one of the systems (surface or subsurface flows)
87 is solved. The integrated approach allows for dynamic evolution of the interconnectivity between
88 the surface water and groundwater systems. This interconnection depends only on the properties
89 of the physical system and governing equations. An indirect approach permits partitioning of the

90 flow components i.e. water and mass fluxes between surface and subsurface systems. The flow
91 components can be solved sequentially. For the groundwater flow solution, ParFlow makes use of
92 an implicit backward Euler scheme in time, and a cell-centered finite-difference scheme in space
93 (Woodward, 1998). An upwind finite-volume scheme in space and an implicit backward Euler
94 scheme in time is used for the overland flow component (Maxwell et al., 2007). ParFlow uses
95 Krylov linear solvers with multigrid preconditioners for the flow equations along with a Newton
96 method for the nonlinearities in the variably saturated flow system (Ashby and Falgout, 1996;
97 Jones and Woodward, 2001). ParFlow’s physically based approach requires a number of
98 parameterizations e.g. subsurface hydraulic properties, such as porosity, the saturated hydraulic
99 conductivity, and the pressure-saturation relationship parameters (relative permeability), etc.
100 (Kollet and Maxwell, 2008a)(Kollet et al., 2010).

101 ParFlow is well documented and has been applied to surface and subsurface flow problems
102 including simulating the dynamic nature of groundwater and surface-subsurface interconnectivity
103 in large domains (e.g. over 600 km²) (e.g. Kollet and Maxwell, 2008; Ferguson and Maxwell,
104 2012; Condon et al., 2013; Condon and Maxwell, 2014), small catchments (e.g. approximately 30
105 km²) (Ashby et al., 1994; Kollet and Maxwell, 2006; Engdahl et al., 2016), complex terrain with
106 highly heterogenous subsurface permeability such as the Rocky Mountain National Park,
107 Colorado, United States (e.g. Engdahl and Maxwell, 2015; Kollet et al., 2017), large watersheds
108 (Abu-El-Sha’r and Rihani, 2007; Kollet et al., 2010), continental scale flows (Condon et al., 2015;
109 Maxwell et al., 2015) and even subsurface–surface and –atmospheric coupling (Maxwell et al.,
110 2011; Williams and Maxwell, 2011; Williams et al., 2013; Gasper et al., 2014; Shrestha et al.,

111 2015). Evidences from these studies suggest ParFlow produce accurate results in simulating flows
112 in surface-subsurface systems in watersheds i.e. the code possesses the capability of performing
113 simulations that accurately represent the behaviors of natural systems on which models are based.

114 The rest of the paper is organized as follows: We provide a brief history of ParFlow’s development
115 in Section 1.1. In Section 2, we describe the core functionality of the code, i.e. the primary
116 functions and the model equations and grid type used by ParFlow. Section 3 covers equation
117 discretization and solvers (e.g. inexact Newton-Krylov, the ParFlow Multigrid (PFMG)
118 preconditioner, and the Multigrid-Preconditioned Conjugate Gradient (MGCG) method) used in
119 ParFlow. Examples of parallel scaling and performance efficiency of ParFlow are revisited in
120 Section 4. The coupling capabilities of ParFlow, with other atmospheric, land surface, and
121 subsurface models are shown in Section 5. We provide a summary and discussion, future directions
122 to the development of ParFlow, and give some concluding remarks in Section 6.

123 1.1 Development History

124 ParFlow development commenced as part of an effort to develop an open–source, object–
125 oriented, parallel watershed flow model initiated by scientists from the Center for Applied
126 Scientific Computing (CASC), Environmental Programs, and the Environmental Protection
127 Department at the Lawrence Livermore National Laboratory (LLNL) in the mid–1990s. ParFlow
128 was born out of this effort to address the need for a code that combines fast, nonlinear solution
129 schemes with massively parallel processing power, and its development continues today (e.g.
130 Ashby et al., 1993; Smith et al., 1995; Woodward, 1998; Maxwell and Miller, 2005; Kollet and

131 Maxwell, 2008; Rihani et al., 2010; Simmer et al., 2015). ParFlow, is now a collaborative effort
132 between numerous institutions including Colorado School of Mines, Research Center Jülich,
133 University of Bonn, Washington State University, the University of Arizona, and Lawrence
134 Livermore National Laboratory, and its working base and development community continues to
135 expand.

136 ParFlow was originally developed for modeling saturated fluid flow and chemical transport
137 in three-dimensional heterogeneous media. Over the past few decades, ParFlow underwent several
138 modifications and expansions (i.e. additional features and capabilities have been implemented)
139 and has seen an exponential growth of applications. For example, a two-dimensional distributed
140 overland flow simulator (surface water component) was implemented into ParFlow (Kollet and
141 Maxwell, 2006) to simulate interaction between surface and subsurface flows. Such additional
142 implementations have resulted in improved numerical methods in the code. ~~It~~ The code's
143 applicability continues to evolve, for example, in recent times, ParFlow has been used in several
144 coupling studies, with subsurface, land surface, and atmospheric models to include physical
145 processes at the land surface (Maxwell and Miller, 2005; Maxwell et al., 2007, 2011; Kollet, 2009;
146 Williams and Maxwell, 2011; Valcke et al., 2012; Valcke, 2013; Shrestha et al., 2014; Beisman et
147 al., 2015) across different spatial scales and resolutions (Kollet and Maxwell, 2008; Condon and
148 Maxwell, 2015; Maxwell et al., 2015). Also, a terrain following mesh formulation has been
149 implemented (Maxwell, 2013) that allows ParFlow to handle problems with fine space
150 discretization near the ground surface that comes with variable vertical discretization flexibility

151 which offer modelers the advantage to increase the resolution of the shallow soil layers (these are
152 discussed in detail below).

153

154 2. Core Functionality of ParFlow

155 The core functionality of the ParFlow model is the solution of three-dimensional variably
156 saturated groundwater flow in heterogeneous porous media ranging from simple domains with
157 minimal topography and/or heterogeneity to highly resolved continental-scale catchments (Jones
158 and Woodward, 2001; Maxwell and Miller, 2005; Kollet and Maxwell, 2008; Maxwell, 2013).
159 Within this range of complexity, the ParFlow model can operate in three different modes: 1).
160 variably saturated; 2). steady-state saturated; and 3). integrated-watershed flows; however, all
161 these modes share a common sparse coefficient matrix solution framework.

162 2.1 Variably Saturated Flow

163 ParFlow can operate in variably saturated mode using the well-known, mixed form of
164 Richards' equation (Celia et al., 1990). The mixed form of Richards' equation implemented in
165 ParFlow is:

$$166 \quad S_s S_w(p) \frac{\partial p}{\partial t} + \phi \frac{\partial(S_w(p))}{\partial t} = \nabla \cdot \mathbf{q} + q_s, \quad (1)$$

$$167 \quad \mathbf{q} = -k_s(\mathbf{x}) k_r(p) \nabla(p - z), \quad (2)$$

168 where S_s is the specific storage coefficient [L^{-1}], S_w is the relative saturation [-] as a function
169 of pressure head p of the fluid/water [L], t is time [T], ϕ is the porosity of the medium [-], \mathbf{q} is

170 the specific volumetric (Darcy) flux [LT^{-1}], k_s is the saturated hydraulic conductivity tensor
171 [LT^{-1}], k_r is the relative permeability [-] which is a function of pressure head, q_s is the general
172 source/sink term [L^3T^{-1}] (includes wells and surface fluxes e.g. evaporation and transpiration),
173 and z is depth below the surface [L]. The Richards' equation assumes that the air phase is infinitely
174 mobile (Richards, 1931). ParFlow has been used to numerically simulate river-aquifer exchange
175 (free-surface flow and subsurface flow), (Frei et al., 2009), and highly heterogenous problems
176 under variably-saturated flow conditions (Woodward, 1998; Jones and Woodward, 2001; Kollet
177 et al., 2010). Under saturated conditions e.g. simulating linear groundwater movement under
178 assumed predevelopment conditions, the steady-state saturated mode can be used.

179

180 2.2 Steady-State Saturated Flow

181 The most basic operational mode is the solution of the steady state, fully saturated
182 groundwater flow equation:

$$183 \quad \nabla \cdot \mathbf{q} - q_s = 0, \quad (3)$$

184 where q_s represents a general source/sink term e.g. wells [L^3T^{-1}], \mathbf{q} is the Darcy' flux [L^2T^{-1}]
185 which is usually written as:

$$186 \quad \mathbf{q} = -k_s \nabla \phi \quad (4)$$

187 where k_s is the saturated hydraulic conductivity [LT^{-1}] and ϕ represents the 3-D hydraulic head-
188 potential [L]. ParFlow does include a direct solution option for the steady state saturated flow that
189 is distinct from the transient solver. For example, ParFlow uses the solver "impes" under single-
190 phase, fully saturated steady state condition relative to the variably saturated, transient mode where

191 Richards' equation solver is used (Maxwell et al., 2016). When studying sophisticated or complex
192 phenomena e.g. simulating fully coupled system (i.e. surface and subsurface flow), an overland
193 flow boundary condition is employed.

194

195 2.3 Overland Flow

196 Surface water systems are connected to the subsurface, and these interactions are
197 particularly important for rivers. However, these connections have been historically difficult to
198 represent explicitly in numerical simulations. A common approach has been to use river routing
199 codes, like HEC, and MODFLOW and its River Package to determine head in the river, which is
200 then used as a boundary condition for the subsurface model. This approach prevents feedbacks
201 between the two models, and a better representation of the physical processes in these kinds of
202 problems is one of the motivations for IHMs. Overland flow is implemented in ParFlow as a two–
203 dimensional kinematic wave equation approximation of the shallow water equations. The
204 continuity equation for two-dimensional shallow overland flow is given as;

$$205 \quad \frac{\partial \psi_s}{\partial t} = \nabla \cdot (\vec{v} \psi_s) + q_s, \quad (5)$$

206 where \vec{v} is the depth averaged velocity vector [LT^{-1}], ψ_s is the surface ponding depth [L], t is time
207 [T], and q_s is a general source/sink (e.g. precipitation rate) [LT^{-1}]. Ignoring the dynamic and
208 diffusion terms results in the momentum equation

$$209 \quad S_{f,i} = S_{o,i}, \quad (6)$$

210 which is known as the kinematic wave approximation. The $S_{f,i}$ and $S_{o,i}$ represent the friction [–]
 211 and bed slopes (gravity forcing term) [–] ~~slopes~~ respectively, where i indicates x – and y –
 212 directions (also shown in equations 7 and 8) (Maxwell et al., 2015). Manning’s equation is used
 213 to generate a flow depth–discharge relationship:

$$214 \quad v_x = \frac{\sqrt{S_{f,x}}}{n} \psi_s^{2/3}, \text{ and} \quad (7)$$

$$215 \quad v_y = \frac{\sqrt{S_{f,y}}}{n} \psi_s^{2/3} \quad (8)$$

216 where n is the Manning’s roughness coefficient [$\text{TL}^{-1/3}$]. Flow of water out of overland flow
 217 simulation domain only occurs horizontally at an outlet which is controlled by specifying a type
 218 of boundary condition at the edge of the simulation domain. In a natural system, the outlet is
 219 usually taken as the region where a river enters another water body such as stream or a lake.

220 ParFlow determines overland flow direction through the D4 flow routing approach. In a simulation
 221 domain, the D4 flow routing approach allows for flow to be assigned from a focal cell to only one
 222 neighboring cell accessed via the steepest or most vertical slope. The shallow overland flow
 223 formulation (equation 9) assumes that the flow depth is averaged-vertically and neglects a vertical
 224 change in momentum in the column of surface water. To account for vertical flow (from the surface
 225 to the subsurface or subsurface to the surface~~into the subsurface from the surface~~), a formulation
 226 that couples the system of equations through a boundary condition at the land surface becomes
 227 necessary. Equation (5) can be modified to include an exchange rate with the subsurface, q_e , as:

$$228 \quad \frac{\partial \psi_s}{\partial t} = \nabla \cdot (\vec{v} \psi_s) + q_s + q_e \quad (9)$$

229 which is common in other IHMs. In ParFlow, the overland flow equations are coupled directly to
 230 Richards' equation at the top boundary cell under saturated conditions. Conditions of continuity
 231 of pressure (i.e. the pressures of the subsurface and surface domains are equal right at the ground
 232 surface) and flux at the top cell of the boundary between the subsurface and surface systems are
 233 assigned ~~(Figure. 1).~~ Figure 1 is provided demonstrating continuity of pressure at the ground
 234 surface for flow from the surface into the subsurface. This assignment is done by setting pressure–
 235 head, in equation (1) equal to the vertically–averaged surface pressure, ψ_s ;

$$236 \quad p = \psi_s = \psi, \quad (10)$$

237 and the flux, q_e equal to the specified boundary conditions (e.g. Neumann or Dirichlet type). For
 238 example, if Neumann type boundary conditions are specified, which are given as;

$$239 \quad q_{BC} = -k_s k_r \nabla(\psi - z) \quad (11)$$

240 and one solves for the flux term in equation (10), the result is;

$$241 \quad q_e = \frac{\partial \|\psi, 0\|}{\partial t} - \nabla \vec{v} \|\psi, 0\| - q_s \quad (12)$$

242 where the $\|\psi, 0\|$ operator is defined as the greater of the quantities, ψ and 0. Substituting equation
 243 (12) for the boundary condition in equation (11), requiring the aforementioned flux continuity

244 $q_{BC} = q_e$, leads to

$$245 \quad -k_s k_r \nabla(\psi - z) = \frac{\partial \|\psi, 0\|}{\partial t} - \nabla \cdot (\vec{v} \|\psi, 0\|) - q_s \quad (13)$$

246 Equation (13) shows that the surface water equations are represented as a boundary condition to
 247 the Richards' equation. That is, the boundary condition links flow processes in the subsurface with
 248 those at the land surface. This boundary condition eliminates the exchange flux and accounts for

249 the movement of the free surface of ponded water at the land surface (Kollet and Maxwell, 2006;
250 Williams and Maxwell, 2011).

251 Many IHMs couple subsurface and surface flows making use of the exchange flux, q_e
252 model. The exchange flux between the domains (the surface and the subsurface) depends on
253 hydraulic conductivity and the gradient across some interface where indirect coupling is used
254 (VanderKwaak, 1999; Panday and Huyakorn, 2004). The exchange flux concept gives a general
255 formulation of a single set of coupled surface-subsurface equations. The exchange flux term, q_e
256 may be included in the shallow overland flow continuity equation as the exchange rate term with
257 the subsurface (equation 9) in a coupled system (Kollet and Maxwell, 2006).

258 Figure. 1 Caption: Coupled surface and subsurface flow systems. Note in this figure the physical
259 system is represented on the left and a schematic of the overland flow boundary condition
260 (continuity of pressure and flux at the ground surface) is on the right. The equation, $p = \psi_s = \psi$
261 in Figure. 1 signifies that the vertically averaged surface pressure and subsurface pressure head are
262 equal right at the land surface.

263

264 2.4 Multi-Phase Flow and Transport Equations

265 Most applications of the code have reflected ParFlow's core functionality as a single-phase
266 flow solver, but there are also embedded capabilities for multi-phase flow of immiscible fluids and
267 solute transport. Multi-phase systems are distinguished from single-phase systems by the presence
268 of one or more interfaces separating the phases, with moving boundaries between phases. The flow

269 equations that are solved in multi-phase systems in a porous medium comprise a set of mass
 270 balance and momentum equations. The equations are given by:

$$271 \quad \frac{\partial}{\partial t} (\phi \rho_i S_i) + \nabla \cdot (\phi \rho_i S_i \vec{v}_i) - \rho_i Q_i = 0, \quad (14)$$

$$272 \quad \phi S_i \vec{v}_i + \lambda_i \cdot (\nabla p_i - \rho_i \vec{g}) = 0, \quad (15)$$

273 where $i = 1, \dots, n$ denotes a given phase (such as air or water). In these equations, ϕ is the intrinsic
 274 medium porosity of the medium [-] which explains the fluid capacity of the porous medium, and
 275 for each phase, i , $S_i(\vec{x}, t)$ is the relative saturation [-] which indicates the content of phase i in
 276 the porous medium, $\vec{v}_i(\vec{x}, t)$ represent Darcy velocity vector [LT⁻¹], $Q_i(\vec{x}, t)$ stands for
 277 source/sink term [T⁻¹], $p_i(\vec{x}, t)$ is the average pressure [ML⁻¹T⁻²], $\rho_i(\vec{x}, t)$ is the mass density
 278 [ML⁻³], λ_i is the mobility [L³TM⁻¹], \vec{g} is the gravity vector [LT⁻²], and \vec{x} and t represent space
 279 vectors and the time respectively. ParFlow solves for the pressures on a discrete mesh and uses a
 280 time-stepping algorithm based on a mass conservative backward Euler scheme and spatial
 281 discretization (a finite volume method). ParFlow's multi-phase flow capability has not been
 282 applied in major studies, however, this capability is also available for testing (Ashby et al., 1993;
 283 Tompson et al., 1994; Falgout et al., 1999; Maxwell et al., 2016).

284 The transport equations included in the ParFlow package describe mass conservation in a
 285 convective flow (no diffusion) with degradation effects and adsorption included along with
 286 extraction and injection wells (Beisman et al., 2015; Maxwell et al., 2016). The transport equation
 287 is defined as follows:

$$\begin{aligned}
288 \quad & \left(\frac{\partial}{\partial t} (\phi c_{i,j}) + \lambda_j \phi c_{i,j} \right) + \nabla \cdot (c_{i,j} \vec{v}) = - \left(\frac{\partial}{\partial t} \left((1 - \phi) \rho_s F_{i,j} \right) + \lambda_i (1 - \phi) \rho_s F_{i,j} \right) + \\
289 \quad & \sum_k^{nI} \gamma_k^{I;i} \chi \Omega_k^I (c_{i,j} - c_{i,j}^{-k}) - \sum_k^{nE} \gamma_k^{E;i} \chi \Omega_k^E c_{i,j} \tag{16}
\end{aligned}$$

290 where ~~ϕ denotes the porosity of the flow medium [-]~~, $c_{i,j}(\vec{x}, t)$ represents concentration
291 fraction of contaminant [-], ~~$\vec{v}(x, t)$ is the Darcy velocity vector [LT⁻¹]~~, λ_i is degradation rate
292 [T⁻¹], $F_i(\vec{x}, t)$ is the mass concentration [L³M⁻¹], $\rho_s(\vec{x})$ is the density of the solid mass [ML⁻³],
293 n_I is injection wells [-], $\gamma_k^{I;i}(t)$ is injection rate [T⁻¹], $\Omega_k^I(\vec{x})$ represent the area of the injection
294 well [-], $c_{i,j}^{-k}(\vec{x}, t)$ is the injected concentration fraction [-], n_E is the extraction wells [-],
295 $\gamma_k^{E;i}(t)$ is extraction rate [T⁻¹], $\Omega_k^E(\vec{x})$ is an extraction well area [-], $i =$
296 $0, \dots, n_{p-1}$ ($n_p \in \{1, 2, 3\}$) is the number of phases, $j = 0, \dots, n_c - 1$ represents the number of
297 contaminants, $c_{i,j}$ is the concentration of contaminant j in phase i , k is hydraulic conductivity
298 [LT⁻¹], $\chi \Omega_k^I$ is the characteristic function of an injection well region, and $\chi \Omega_k^E$ is the characteristic
299 function of an extraction well region. The mass concentration term, $F_{i,j}$ is taken to be instantaneous
300 in time and a linear function of contaminant concentration:

$$301 \quad F_{i,j} = K_{d,j} c_{i,j} \tag{17}$$

302 where $K_{d,j}$ is the distribution coefficient of the component [L³M⁻¹]. The transport/advection
303 equation or convective flow calculation performed by ParFlow offers a choice of a first-order
304 explicit upwind scheme or a second-order explicit Godunov scheme. The advection calculations
305 are discretized as boundary value problems for each primary dimension over each compute cell.
306 The discretization is a fully-explicit, forward Euler first-order accurate in time approach. The
307 implementation of a second-order explicit Godunov scheme (second-order advection scheme)

308 minimizes numerical dispersion and presents accurate computational process at these time scales
309 than either an implicit or lower-order explicit scheme. Stability issue here is that the simulation
310 timestep is restricted via the Courant-Friedrichs-Lewy (CFL) condition, which demands that time
311 steps are chosen small enough to ensure that mass not be transported more than one grid cell in a
312 single timestep in order to maintain stability (Beisman, 2007).

313

314 2.5 Computational Grids

315 An accurate numerical approximation of a set of partial differential equations is strongly
316 dependent on the simulation grid. Integrated hydrologic models can use unstructured or structured
317 meshes for the discretization of the governing equations. The choice of grid type to adopt is
318 problem-specific and often a subjective choice since the same domain can be represented in many
319 ways, but there are some clear tradeoffs. For example, structured grid models, such as ParFlow,
320 may be preferred to unstructured grid models because structured grids provide significant
321 advantages in computational simplicity and speed, and are amenable to efficient parallelization
322 (Durbin, 2002; Kumar et al., 2009; Osei-Kuffuor et al., 2014). ParFlow adopts a regular, structured
323 grid specifically for its parallel performance. There are currently two regular grid formulations
324 included in ParFlow, an orthogonal grid and a terrain-following formulation (TFG); both allow for
325 variable vertical discretization (thickness over an entire layer) over the domain.

326 2.5.1 Orthogonal Grid

327 Orthogonal grids have many advantages, and many approaches are available to transform
328 an irregular grid into an orthogonal grid such as conformal mapping. This mapping defines a

329 transformed set of partial differential equations using an elliptical system with “control functions”
330 determined in such a way that the generated grid would be either orthogonal or nearly orthogonal.
331 However, conformal mapping may not allow flexibility in the control of the grid node distribution,
332 which diminishes its usefulness with complex geometries (Mobley and Stewart, 1980; Haussling
333 and Coleman, 1981; Visbal and Knight, 1982; Ryskin and Leal, 1983; Allievi and Calisal, 1992;
334 Eca, 1996).

335 A Cartesian, regular, orthogonal grid formulation is implemented by default in ParFlow,
336 though some adaptive meshing capabilities are still included in the source code. For example,
337 layers within a simulation domain can be made to have varying thickness. The upper portion of
338 Figure 2 shows the standard way topography or any other non-rectangular domain boundaries are
339 represented in ParFlow. The domain limits, and any other internal boundaries, can be defined using
340 grid-independent triangulated irregular network (TIN) files that define a geometry, or a gridded
341 indicator file can be used to define geometric elements. ParFlow uses octree space partitioning
342 algorithm (a grid-based algorithm or mesh generators filled with structured grids) (Maxwell, 2013)
343 to depict complex structures/land surface representations (e.g. topography, watershed boundaries,
344 and different hydrologic facies) in three-dimensional space (Kollet et al., 2010). These land surface
345 features are mapped onto the orthogonal grid, and looping structures that encompass these irregular
346 shapes are constructed (Ashby et al., 1997). The grid cells above ground surface are inactive
347 (shown in upper region of Figure 2) and are stored in the solution vector but not included in the
348 solution.

349 2.5.2 Terrain Following Grid

350 The inactive portion of a watershed defined with an orthogonal grid can be quite large in
351 complex watersheds with high-relief. In these cases, it is advantageous to use a grid that allows
352 these regions to be omitted. ParFlow's structured grid conforms to the topography via
353 transformation by the terrain following grid formulation. This transform alters the form of Darcy's
354 law to incorporate a topographic slope component. For example, subsurface fluxes are computed
355 separately in both x and y directions making use of the terrain following grid transform as:

$$356 \quad q_x = K \sin(\theta_x) + K \frac{\partial p}{\partial y} \cos(\theta_x), \text{ and}$$
$$357 \quad q_y = K \sin(\theta_y) + K \frac{\partial p}{\partial x} \cos(\theta_y) \quad (18)$$

358 where q_x and q_y represent source/sink terms, such as fluxes, that include potential recharge flux
359 at the ground surface [LT^{-1}], p is the pressure head [L]; K is the saturated hydraulic conductivity
360 tensor, [LT^{-1}], θ is the local angle [–] of topographic slope, S_x and S_y in the x and y directions
361 and may be presented as $\theta_x = \tan^{-1} S_x$ and $\theta_y = \tan^{-1} S_y$ respectively (Weill et al., 2009). The
362 terrain following grid formulation comes handy when solving coupled surface and subsurface
363 flows (Maxwell, 2013). The terrain following grid formulation uses the same surface slopes
364 specified for overland flow to transform the grid, whereas the slopes specified in the orthogonal
365 grid are only used for 2-D overland flow routing and do not impact the subsurface formulation
366 (see Figure 2). Note that TIN files can still be used to deactivate portions of the transformed
367 domain.

368

369 Figure 2 Caption: Representation of orthogonal (upper) and the terrain following (lower) grid
370 formulations and schematics of the related finite difference dependences (left). The i, j , and k are
371 the x, y , and z cell indices

372

373 3. Equation Discretization and Solvers

374 The core of the ParFlow code is its library of numerical solvers. As noted above, in most
375 cases, the temporal discretization of the governing equations uses an implicit (backward Euler)
376 scheme; with cell-centered finite differences in spatial dimensions. Different components of this
377 solution framework have been developed for the various operational modes of ParFlow including
378 an inexact Newton-Krylov nonlinear solver (section 3.1), a multigrid algorithm (section 3.2), and
379 a multigrid-preconditioned conjugate gradient (MGCG) solver in (section 3.3). The conditions,
380 requirements, and constraints on the solvers depend on the specifics of the problem being solved,
381 and some solvers tend to be more efficient (faster overall convergence) than others for a given
382 problem. The core structure of these solvers and some of their implementation details are given
383 below, with an emphasis on the main concepts behind each solver.

384

385 3.1 Newton–Krylov solver for Variably Saturated Flow

386 The cell-centered fully-implicit discretization scheme applied to Richards' equation leads
387 to a set of coupled discrete nonlinear equations that need to be solved at each time step, and, for
388 variably saturated subsurface flow, ParFlow does this with the inexact Newton-Krylov method

389 implemented in the KINSOL package (Hindmarsh et al., 2005; Collier et al., 2015). Newton-
390 Krylov methods were initially utilized in the context of partial differential equations by (Brown
391 and Saad, 1990). In the approach, coupled nonlinear system as a result of discretization of the
392 partial differential equation is solved iteratively. Within each iteration, the nonlinear system is
393 linearized via a Taylor expansion. After linearization, an iterative Krylov method is used to solve
394 the resulting linear Jacobian system (Woodward, 1998; Osei-Kuffuor et al., 2014). For variably
395 saturated subsurface flow, ParFlow uses the GMRES Krylov method (Saad and Schultz, 1986).
396 Figure 3 is a flow chart of the solution technique ParFlow uses to provide approximate solutions
397 to systems of nonlinear equations.

398

399 Figure 3 caption: Working flow chart of ParFlow's solver for linear and non-linear system solution

400

401 The benefit of this Newton-Krylov method is that the Krylov linear solver requires only
402 matrix-vector products. Because the system matrix is the Jacobian of the nonlinear function, these
403 matrix-vector products may be approximated by taking directional derivatives of the nonlinear
404 function in the direction of the vector to be multiplied. This approximation is the main advantage
405 of the Newton-Krylov approach as it removes the requirement for matrix entries in the linear
406 solver. An inexact Newton method is derived from a Newton method by using an approximate
407 linear solver at each nonlinear iteration, as is done in the Newton-Krylov method (Dembo et al.,
408 1982; Dennis and Schabel, 1996). This approach takes advantage of the fact that when the
409 nonlinear system is far from converged, the linear model used to update the solution is a poor

410 approximation. Thus, the convergence criteria of early linear system solve is relaxed. The tolerance
411 required for solution of the linear system is decreased as the nonlinear function residuals approach
412 zero. The convergence rate of the resulting nonlinear solver can be linear or quadratic, depending
413 on the algorithm used. Through the KINSOL package, ParFlow can either use a constant tolerance
414 factor or ones from (Eisenstat and Walker, 1996). Krylov methods can be very robust, but they
415 can be slow to converge. As a result, it is often necessary to implement a preconditioner, or
416 accelerator, for these solvers.

417

418 3.2 Multigrid Solver

419 Multigrid (MG) methods constitute a class of techniques or algorithms for solving
420 differential equations (system of equations) using a hierarchy of discretization (Volker, 1987;
421 Briggs et al., 2000). Multigrid algorithms are applied primarily to solve linear and nonlinear
422 boundary value problems and can be used as either preconditioners or solvers. The most efficient
423 method for preconditioning the linear systems in ParFlow is the ParFlow Multigrid algorithm
424 (PFMG) (Ashby and Falgout, 1996; Jones and Woodward, 2001). Multigrid algorithms arise from
425 discretization of elliptic partial differential equations (Briggs et al., 2000), and, in ideal cases, have
426 convergence rates that do not depend on the problem size. In these cases, the number of iterations
427 remains constant even as problems sizes grow large. Thus, the algorithm is algorithmically
428 scalable. However, it may take longer to evaluate each iteration as problem sizes increase. As a
429 result, ParFlow utilizes the highly efficient implementation of PFMG in the hypre library (Falgout
430 and Yang, 2002).

431 For variably saturated subsurface flow, ParFlow uses the Newton-Krylov method coupled
432 with a multigrid preconditioner to accurately solve for the water pressure (hydraulic head) in the
433 subsurface and diagnoses the saturation field (which is used in determining the water table).
434 (Woodward, 1998; Jones and Woodward, 2000, 2001; Kollet et al., 2010). The water table is
435 calculated for computational cells having hydraulic heads above the bottom of the cells. Generally,
436 a cell is saturated if the hydraulic head in the cell is above the node elevation (cell center) or the
437 cell is unsaturated if the hydraulic head in the cell is below the node elevation. For saturated flow,
438 ParFlow uses the conjugate gradient method also coupled with a multigrid method. It is important
439 to note that subsurface flow systems are usually much larger radially than they are thick, so it is
440 common for the computational grids to have highly anisotropic cell aspect ratios to balance the
441 lateral and vertical discretization. Combined with anisotropy in the permeability field, these high
442 aspect ratios produce numerical anisotropy in the problem, which can cause the multigrid
443 algorithms to converge slowly (Jones and Woodward, 2001). To correct this problem, a
444 semicoarsening strategy or algorithm is employed, where the grid is coarsened in one direction at
445 a time. The direction chosen is the one with the smallest grid spacing i.e. the tightest coupling. In
446 an instance where more than one direction has the same minimum spacing, then the algorithm
447 chooses the direction in the order of x , followed by y , and then in z . To decide on how and when
448 to terminate the coarsening algorithm, Ashby and Falgout (1996) determined that a
449 semicoarsening down to a $(1 \times 1 \times 1)$ grid is ideal for groundwater problems.

450

451 3.3 Multigrid-Preconditioned Conjugate Gradient (MGCG)

452 ParFlow uses the multigrid-preconditioned conjugate gradient (CG) solver to solve the
453 groundwater equations under steady-state, and fully saturated flow conditions (Ashby and Falgout,
454 1996). These problems are symmetric and positive definite, two properties for which the CG
455 method was designed to target. While CG lends itself to efficient implementations, the number of
456 iterations required to solve a system such as results from discretization of the saturated flow
457 equation increases as the problem size grows. The PFMG multigrid algorithm is used as a
458 preconditioner to combat this growth and results in an algorithm for which the number of iterations
459 required to solve the system grows only minimally. See Ashby and Falgout (1996) for a detailed
460 description of these solvers and the parallel implementation of the multigrid preconditioned CG
461 method in ParFlow (Gasper et al., 2014; Osei-Kuffuor et al., 2014).

462

463 3.4 Preconditioned Newton-Krylov for Coupled Subsurface – Surface Flows

464 As discussed above, coupling between subsurface and surface or overland flow in
465 ParFlow is activated by specifying an overland boundary condition at the top surface of the
466 computational domain, but this mode of coupling allows for activation and deactivation of the
467 overland boundary condition during simulations where ponding or drying occur. Thus, surface-
468 subsurface coupling can occur anywhere in the domain during a simulation and it can change
469 dynamically during the simulation. Overland flow may occur by the Dunne or Horton mechanism
470 depending on local dynamics. Overland flow routing is enabled when the subsurface cells are fully
471 saturated. As discussed above, i
472 n ParFlow the coupling between the subsurface and surface flows
is handled implicitly. ParFlow solves this implicit system with the inexact Newton-Krylov method

473 described above. However, in this case, the preconditioning matrix is adjusted to include terms
474 from the surface coupling. In the standard saturated or variably saturated case, the multigrid
475 method is given the linear system matrix, or a symmetric version, resulting from discretization of
476 the subsurface model. Because ParFlow uses a structured mesh, these matrices have a defined
477 structure making their evaluation and application of multigrid straightforward. Due to varying
478 topographic height of the surface boundary, where the surface coupling is enforced, the surface
479 effects add non-structured entries in the linear system matrices. These entries increase complexity
480 of the matrix entry evaluations and reduce effectiveness of the multigrid preconditioner. In this
481 case, the matrix-vector products are most effectively performed through computation of the linear
482 system entries, rather than the finite difference approximation to the directional derivative. For
483 the preconditioning, surface couplings are only included if they model flow between cells at the
484 same vertical height i.e. in situations where overland flow boundary conditions are imposed or
485 activated.- This restriction maintains the structured property of the preconditioning matrix while
486 still including much of the surface coupling in the preconditioner. Both these adjustments led to
487 considerable speedup in coupled simulations (Osei-Kuffuor et al., 2014).

488

489 4. Parallel Performance Efficiency

490 Scaling efficiency metrics offer a quantitative method for evaluating the performance of
491 any parallel model. Good scaling generally means that the efficiency of the code is maintained as
492 the solution of the system of equations is distributed onto more processors or as the problem
493 resolution is refined and processing resources are added. Scalability can depend on the problem

494 size, the processor number, the computing environment, and the inherent capabilities of the
495 computational platform used e.g. choice of a solver. The performance of ParFlow (or any parallel
496 code) is typically determined through weak and strong scaling (Gustafson, 1988). Weak scaling
497 involves the measurement of code's efficiency in solving problems of increasing size (i.e.
498 describes how the solution time change with change in the number of processors for a fixed
499 problem size per processor). In weak scaling, the simulation time should remain constant, as the
500 size of the problem and number of processing elements grow such that the same amount of work
501 is conducted on each processing element. Following Gustafson (1988), scaled parallel efficiency
502 is given by:

$$503 \quad E(n, p) = \frac{T(n, 1)}{T(pn, p)} \quad (19)$$

504 where $E(n, p)$ denotes parallel efficiency, T represents the run time as a function of the problem
505 size n , which is spread across several processors p . Parallel code is said to be perfectly efficient if
506 $E(n, p) = 1$, and the efficiency decreases as $E(n, p)$ approaches 0. Generally, parallel efficiency
507 decreases with increasing processor number as communication overhead between
508 nodes/processors becomes the limiting factor.

509 Strong scaling describes the measurement of how much the simulation or solution time
510 changes with the number of processors for a given problem of fixed total size (Amdahl, 1967). In
511 strong scaling, a fixed size task is solved on a growing number of processors, and the associated
512 time needed for the model to compute the solution is determined (Woodward, 1998; Jones and
513 Woodward, [2000](#)). If the computational time decreases linearly with the processor number, a

514 perfect parallel efficiency, ($E = 1$) results. The value of E is determined using equation (19).

515 ParFlow has been shown to have excellent parallel performance efficiency, even for large problem

516 sizes and processor counts (see Table 1) (Ashby and Falgout, 1996; Kollet and Maxwell, 2006).

517 In situations where ParFlow works in conjunction with or coupled to other subsurface, land surface

518 or atmospheric models (see Section 5) i.e. increased computational complexity by adding different

519 components or processes, improved computational time may not only depend on ParFlow. The

520 computational cost of such an integrated model is extremely difficult to predict because of the

521 nonlinear nature of the system. The solution time may depend on number of factors including the

522 number of degrees of freedom, the heterogeneity of the parameters, which processes are active

523 (e.g. snow accumulation compared to nonlinear snowmelt processes in land surface model or the

524 switching on or off of the overland flow routing in ParFlow). The only way to know how fast a

525 specific problem will run is to try that problem. Many of the studies presented in Table 1 include

526 computational times for problems with different complexities where ParFlow was used. In a

527 scaling study with ParFlow, Maxwell (2013)— examined the relative performance of

528 preconditioning the coupled variably saturated subsurface and surface flow system with the

529 symmetric portion or full matrix for the system. Both options use ParFlow’s multigrid

530 preconditioner. Solver performance was demonstrated by combining the analytical Jacobian and

531 the non-symmetric linear preconditioner. The study showed that the non-symmetric linear

532 preconditioner presents faster computational times and efficient scaling gains. A section of the

533 study results is reproduced in Table 1, in addition to other scaling studies demonstrating ParFlow’s

534 parallel efficiency. This tradeoff was also examined in Jones and Woodward (2000).

535 It is worth noting that large and/or complex problem sizes (e.g. simulating a large
536 heterogenous domain size with over 8.1 billion unknowns) will always take time to solve directly,
537 but the approach for setting up a problem depends on the specific problem being modeled. Even
538 for one specific kind of model there may be multiple workflows and how to model such complexity
539 becomes sole responsibility of the modeler. The studies involving ParFlow outlined in Table 1
540 provide a wealth of knowledge regarding domain setup for problems of different complexities.
541 Since these are all specific applications, their information will likely be very useful to modelers
542 trying to build a new domain during the setup and planning phases.

543

544 Table 1: Details for the various parallel scaling studies conducted using ParFlow.

545

546 5. Coupling

547 Different integrated models including atmospheric or weather prediction models (e.g. Weather
548 Research Forecasting Model, Advanced Regional Prediction System, Consortium for Small-Scale
549 Modeling), land surface models (e.g. Common Land Model, Noah Land Surface Model), and a
550 subsurface model (e.g. CruchFlow) have been coupled with ParFlow to simulate a variety of
551 coupled earth system effects (see Figure 4(a)). Coupling between ParFlow and other integrated
552 models was performed to better understand the physical processes that occur at the interfaces
553 between the deeper subsurface and ground surface, and between the ground surface and the
554 atmosphere. None of the individual models can achieve this on their own because ParFlow cannot

555 account for land surface processes (e.g. evaporation), and atmospheric and land surface models
556 generally do not simulate deeper subsurface flows (Ren and Xue, 2004; Chow et al., 2006;
557 Beisman, 2007; Maxwell et al., 2007; Shi et al., 2014). Model coupling can be achieved either via
558 “offline coupling” where models involved in the coupling process are run sequentially and
559 interactions between them is one-way (i.e. information is only transmitted from one model to the
560 other) or “online” where they interact and feedback mechanisms among components are
561 represented (Meehl et al., 2005; Valcke et al., 2009). Each of the coupled models uses its own
562 solver for the physical system it is solving, then information is passed between the models. As
563 long as each model exhibits good parallel performance, this approach still allows for simulations
564 at very high resolution, with a large number of processes (Beven, 2004; Ferguson and Maxwell,
565 2010; Shen and Phanikumar, 2010; Shi et al., 2014). This section focuses on the major couplings
566 between ParFlow and other codes. We point out specific functions of the individual models as
567 stand-alone codes that are relevant to the coupling process. In addition, information about the role
568 or contribution of each model at the coupling interface (see Figure 4(b)) that connects with
569 ParFlow are presented (Figure 5 shows the communication network of the coupled models). We
570 discuss couplings between ParFlow and its land surface model (a modified version of the original
571 Common Land Model introduced by Dai et al., (2003)), Consortium for Small-Scale Modeling
572 (COSMO), Weather Research Forecasting Model, Advanced Regional Prediction System, and
573 CruchFlow in sections 5.1, 5.2, 5.3, 5.4, and 5.5 respectively.

574 Figure 4(a) Caption: A pictorial description of the relevant physical environmental features and
575 model coupling. CLM represents the Community Land Model, a stand-alone Land Surface Model

576 (LSM) via which ParFlow couples' COSMO. The modified version of CLM by Dai et al., (2003)
577 and is not shown in Figure 4(a) because it is a module only for ParFlow, not really a stand-alone
578 LSM any longer.

579

580 Figure 4(b) Caption: Schematic showing information transmission at the coupling interface. PF,
581 LSM, and ATM indicate the portions of the physical system simulated by ParFlow, Land Surface
582 Models, and Atmospheric Models respectively. The downward and upward arrows indicate the
583 directions of information transmission between adjacent models. Note: Coupling between ParFlow
584 and CrunchFlow (not shown) occur within the subsurface.

585 5.1 ParFlow–Common Land Model (PF.CLM)

586 The Common Land Model (CLM) is a land surface model designed to complete land-
587 water-energy balance at the land surface (Dai et al., 2003). CLM parameterizes the moisture,
588 energy and momentum balances at the land surface and includes a variety of customizable land
589 surface characteristics and modules, including land surface type (land cover type, soil texture, and
590 soil color), vegetation and soil properties (e.g. canopy roughness, zero-plane displacement, leaf
591 dimension, rooting depths, specific heat capacity of dry soil, thermal conductivity of dry soil,
592 porosity), optical properties (e.g. albedos of thick canopy), and physiological properties related to
593 the functioning of the photosynthesis-conductance model (e.g. green leaf area, dead leaf, and stem
594 area indices). A combination of numerical schemes is employed to solve the governing equations.
595 CLM uses a time integration scheme which proceeds by a split-hybrid approach, where the solution
596 procedure is split into “energy balance” and “water balance” phases in a very modularized structure

597 (Mikkelsen et al., 2013; Steiner et al., 2005, 2009). The CLM described here and as incorporated
 598 in ParFlow is a modified version of the original CLM introduced by Dai et al., (2003), though the
 599 original version was coupled to ParFlow in previous model applications (e.g. Maxwell and Miller,
 600 2005). The current coupled model, PF.CLM consist of ParFlow incorporated with land surface
 601 model Jefferson et al., (2015), (2017), and Jefferson and Maxwell, (2015).This results in the
 602 coupled model, PF.CLM i.e. ParFlow with its own land surface model. The modified CLM is
 603 composed of a series of land surface modules that are called as a subroutine within ParFlow to
 604 compute energy and water fluxes (e.g. evaporation and transpiration) to and out of the soil. For
 605 example, the modified CLM computes bare ground surface evaporative flux, E_{gr} as

$$606 \quad E_{gr} = -\beta \rho_a u_* q_* \quad (20)$$

607 where β (dimensionless) denotes soil resistance factor, ρ_a represents air density [ML^{-3}], u_*
 608 represents friction velocity [LT^{-1}], and q_* (dimensionless) stands for humidity scaling parameter
 609 (Jefferson and Maxwell, 2015). Evapotranspiration for vegetated land surface, E_{veg} is computed
 610 as

$$611 \quad E_{veg} = [R_{pp,dry} + L_w] L_{SAI} \left[\frac{\rho_a}{r_b} (q_{sat} - q_{af}) \right] \quad (21)$$

612 where r_b is the air density boundary resistance factor [LT^{-1}], q_{sat} (dimensionless) is saturated
 613 humidity at the land surface, and q_{af} (dimensionless) is the canopy humidity. Combination of q_{sat}
 614 and q_{af} forms the potential evapotranspiration. The potential evapotranspiration is divided into
 615 transpiration $R_{pp,dry}$ (dimensionless) which depends on the dry fraction of the canopy, and
 616 evaporation from foliage covered by water L_w (dimensionless). L_{SAI} (dimensionless) is summation

617 of the leaf and stem area indices which estimates the total surface from which evaporation can
618 occur. A detailed description of the equations CLM of PF.CLM uses can be found in Jefferson et
619 al., (2015), (2017), and Jefferson and Maxwell, (2015).

620 ~~The coupled model~~ PF.CLM simulates variably saturated subsurface flow, surface or
621 overland flow, and above-ground processes. PF.CLM was developed prior to the current
622 community land model (see section 5.2), and the module structure of the current and early versions
623 are different. PF.CLM has been updated over the years to improve its capabilities. PF.CLM was
624 first done in the early 2000's, as an undiversified, a column proof-of-concept model, where data
625 or message was transmitted between the coupled models via input/output files (Maxwell and
626 Miller, 2005). Later, PF.CLM was presented in a distributed or diversified approach with a parallel
627 input/output file structure where CLM is called as a set sequence of steps within ParFlow (Kollet
628 and Maxwell, 2008a). These modifications, for example, were done to incorporate subsurface
629 pressure values from ParFlow into chosen computations (Jefferson and Maxwell, 2015). These, to
630 some extent differentiate the modified version (PF.CLM) from the original CLM by Dai et al.,
631 (2003). Within the coupled PF.CLM, ParFlow solves the governing equations for overland and
632 subsurface flow systems and the CLM modules add the energy balance and mass fluxes from the
633 soil, canopy, and root zone that can occur (i.e. interception, evapotranspiration etc.) (~~Maxwell and~~
634 ~~Miller, 2005)~~(Jefferson and Maxwell, 2015).

635 At the coupling interface where the models overlap and undergo online
636 communication~~communicate~~ (see Figure 4(b)), ParFlow calculates and passes soil moisture as well
637 as pressure heads of the subsurface to CLM, and CLM calculates and transmits transpiration from

638 plants, canopy and ground surface evaporation, snow accumulation and melt, and infiltration from
639 precipitation to ParFlow (Ferguson et al., 2016). In short, CLM does all canopy water balances
640 and snow, but once the water through falls to the ground, or snow melts, ParFlow takes over and
641 estimates the water balances via the nonlinear Richards' equation. The coupled model, PF.CLM,
642 has been shown to more accurately predict root-depth soil moisture compared to the uncoupled
643 model i.e. stand-alone land surface model (CLM) with capability of computing near surface soil
644 moisture. This increased accuracy results from the coupling of soil saturations determined by
645 ParFlow and their impacts on other processes including runoff and infiltration (Kollet, 2009;
646 Shrestha et al., 2014; Gebler et al., 2015; Gilbert and Maxwell, 2016). For example, (Maxwell and
647 Miller, 2005) found that simulations of deeper soil saturation (more than 40cm) vary between
648 PF.CLM and uncoupled models, with PF.CLM simulations closely matching the observed data.
649 Table 2 contains summaries of studies conducted with ParFlow coupled to either the original
650 version of CLM by (Dai et al., 2003) or modified CLM (ParFlow with land surface model).

651 5.1.1. ParFlowE–Common Land Model (ParFlowE[CLM])

652 It is well established that ParFlow in conjunction with CLM ~~PF.CLM~~ does perform well in
653 estimating all canopy water and subsurface water balances (Maxwell and Miller, 2005; Mikkelsen
654 et al., 2013; Ferguson et al., 2016). ParFlow, as a component of the coupled model has been
655 modified into a new parallel numerical model, ParFlowE to incorporate the more complete heat
656 equation coupled to variably saturated flow. ParFlowE simulates coupling of terrestrial hydrologic
657 and energy cycles i.e. coupled moisture, heat, and vapor transport in the subsurface. ParFlowE is
658 based on the original version of ParFlow having identical solution schemes and coupling approach

659 with CLM. A coupled three-dimensional subsurface heat transport equation is implemented in
660 ParFlowE using a cell-centered finite difference scheme in space and an implicit backward Euler
661 differencing scheme in time. However, the solution algorithm employed in ParFlow is fully
662 exploited in ParFlowE where the solution vector of the Newton-Krylov method was extended to
663 two dimensions (Kollet et al., 2009). In some integrated and climate models, the convection term
664 of subsurface heat flux and the effect of soil moisture on energy transport is neglected due to
665 simplified parameterizations and computational limitations. However, both convection and
666 conduction terms are considered in ParFlowE (Khorsandi et al., 2014). In ParFlowE, functional
667 relationships (i.e. equations of state) are performed to relate density and viscosity to temperature
668 and pressure, and thermal conductivity to saturation. That is, modeling thermal flows by relating
669 these parameterizations in simulating heat flow is an essential component of ParFlowE. In
670 coupling between ParFlowE and CLM, ParFlowE[CLM], the one-dimensional subsurface heat
671 transport in the CLM is replaced by the three-dimensional heat transport equation including the
672 process of convection of ParFlowE. CLM computes mass and energy balances at ground surface
673 that lead to moisture fluxes and pass these fluxes to the subsurface moisture algorithm of
674 ParFlowE[CLM]. These fluxes are used in computing subsurface moisture and temperature fields
675 which are then passed back to the CLM.

676

677 5.2 ParFlow in the Terrestrial Systems Modeling Platform, TerrSysMP

678 ParFlow is part of the Terrestrial System Modeling Platform TerrSysMP, which comprise
679 the nonhydrostatic fully compressible limited-area atmospheric prediction model, COSMO,

680 designed for both operational numerical weather prediction and various scientific applications on
681 the meso- β (horizontal scales of 20–200km) and meso- γ (horizontal scales of 2–20km) (Duniec
682 and Mazur, 2011; Levis and Jaeger, 2011; Bettems et al., 2015), and the Community Land Model
683 version 3.5 (CLM3.5). Currently, it is used in direct simulations of severe weather events triggered
684 by deep moist convection, including intense mesoscale convective complexes, prefrontal squall-
685 line storms, supercell thunderstorms, and heavy snowfall from wintertime mesocyclones. COSMO
686 solves nonhydrostatic, fully compressible hydro-thermodynamical equations in advection form
687 using the traditional finite difference method (Vogel et al., 2009; Mironov et al., 2010; Baldauf et
688 el., 2011; Wagner et al., 2016).

689 [An online c](#)Coupling between ParFlow and the COSMO model is performed via CLM3.5
690 (Gasper et al., 2014; Shrestha et al., 2014; Keune et al., 2016). Similar to the Common Land Model
691 (by (Dai et al., 2003)), CLM3.5 module accounts for surface moisture, carbon, and energy fluxes
692 between the shallow or near-surface soil (discretized/specified top soil layer), snow, and the
693 atmosphere (Oleson et al., 2008). The model components of a fully coupled system consisting of
694 COSMO, CLM3.5, and ParFlow are assembled by making use of the multiple-executable
695 approach (e.g. with OASIS3-MCT model coupler). The OASIS3-MCT coupler employs
696 communication strategies based on the message passing interface standards, MPI1/MPI2 and the
697 Project for Integrated Earth System Modeling, PRISM, Model Interface Library (PSMILe) for
698 parallel communication of two-dimensional arrays between OASIS3-MCT coupler and the
699 coupling models (Valcke et al., 2012; Valcke, 2013). The OASIS3-MCT specifies the series of
700 coupling, frequency of the couplings, the coupling fields, the spatial grid of the coupling fields,

701 transformation type of the (two-dimensional) coupled fields, and simulation time management and
702 integration.

703 At the coupling interface, the OASIS3-MCT interface interchanges the atmospheric
704 forcing terms and the surface fluxes in serial mode. The lowest level and current time step of the
705 atmospheric state of COSMO is used as the forcing term for CLM3.5. CLM3.5 then computes and
706 returns the surface energy and momentum fluxes, outgoing longwave radiation, and albedo to
707 COSMO (Baldauf et al., 2011). The air temperature, wind speed, specific humidity, convective
708 and grid-scale precipitation, pressure, incoming shortwave (direct and diffuse) and longwave
709 radiation, and measurement height are sent from COSMO to CLM3.5. In CLM3.5, a mosaic/tilling
710 approach may be used to represent the subgrid-scale variability of land surface characteristics,
711 which considers a certain number of patches/tiles within a grid cell. The surface fluxes and surface
712 state variables are first calculated for each tile and then spatially averaged over the whole grid cell
713 (Shrestha et al., 2014) . As with PF.CLM3.5, the one-dimensional soil column moisture predicted
714 by CLM3.5 gets replaced by ParFlow's variably saturated flow solver, so ParFlow is responsible
715 for all calculations relating soil moisture redistribution and groundwater flow. Within the
716 OASIS3-MCT ParFlow sends the calculated pressure and relative saturation for the coupled region
717 soil layers to CLM3.5. The CLM3.5 also transmits depth-differentiated source and sink terms for
718 soil moisture including soil moisture flux e.g. precipitation, and soil evapotranspiration for the
719 coupled region soil layers to ParFlow. Applications of TerrSysMP in fully coupled mode from
720 saturated subsurface across the ground surface into the atmosphere include a study on the impact

721 of groundwater on the European heat wave 2003 and the influence of anthropogenic water use on
722 the robustness of the continental sink for atmospheric moisture content (Keune et al., 2016).

723 5.3 ParFlow–Weather Research Forecasting models (PF.WRF)

724 The Weather Research and Forecast (WRF) is a mesoscale numerical weather prediction
725 system designed to be flexible and efficient in a massively parallel computing architecture. WRF
726 is a widely used model that provides a common framework for idealized dynamical studies, full
727 physics numerical weather prediction, air-quality simulations, and regional climate simulations
728 (Michalakes et al., 1999, 2001; Skamarock et al., 2005). The model contains numerous mesoscale
729 physics options such as microphysics parameterizations (including explicitly resolved water vapor,
730 cloud, and precipitation processes), surface layer physics, shortwave radiation, longwave
731 radiation, land surface, planetary boundary layer, data assimilation, and other physics and
732 dynamics alternatives suitable for both large-eddy and global-scale simulations. Similar to
733 COSMO, the WRF model is a fully compressible, conservative-form, non-hydrostatic atmospheric
734 model which uses time-splitting integration techniques (discussed below) to efficiently integrate
735 the Euler equations (Skamarock and Klemp, 2007).

736 The [online](#) ParFlow WRF coupling (PF.WRF) extends the WRF platform down to bedrock
737 by including highly resolved three-dimensional groundwater and variably saturated shallow or
738 deep vadose zone flows, and a fully integrated lateral flow above ground surface (Molders and
739 Ruhaak, 2002; Seuffert et al., 2002; Anyah et al., 2008; Maxwell et al., 2011). The land surface
740 model portion that links ParFlow to WRF is supplied by WRF through its land surface component,
741 the Noah Land Surface Model (Ek et al., 2003); the standalone version of WRF has no explicit

742 model of subsurface flow. Energy and moisture fluxes from the land surface are transmitted
 743 between the two models via the Noah LSM which accounts for the coupling interface, and which
 744 is conceptually identical to the coupling in PF-COSMO. The three-dimensional variably saturated
 745 subsurface and two-dimensional overland flow equations, and the three-dimensional atmospheric
 746 equations given by ParFlow and WRF are simultaneously solved by the individual model solvers.
 747 Land surface processes, such as evapotranspiration, are determined in the Noah LSM as a function
 748 of potential evaporation and vegetation fraction. This effect is calculated with the formulation:

$$749 \quad E(x) = F^{f_x}(1 - f_{avg})E_{pot} \quad (22)$$

750 where $E(x)$ stands for rate of soil evapotranspiration (length per unit time), f_x represents empirical
 751 coefficient, f_{avg} denotes vegetation fraction, and E_{pot} is potential evaporation, determined that
 752 depends on atmospheric conditions from the WRF boundary layer parameterization (Ek et al.,
 753 2003). The vegetation fraction is zero over bare soils (i.e. only soil evaporation), so equation 22
 754 becomes:

$$755 \quad E(x) = F^{f_x}E_{pot} \quad (23)$$

756 The quantity F is parameterized as follows:

$$757 \quad F = \frac{\phi S_w - \phi S_{res}}{\phi - \phi S_{res}}, \quad (24)$$

758 where ϕ is the porosity of the medium, S_w and S_{res} are relative saturation and residual saturation
 759 respectively, from vanGenuchten relationships (VanGenuchten, 1980; Williams and Maxwell,
 760 2011). Basically, F refers to the parameterization of the interrelationship between evaporation and

761 near-ground soil water content and provides one of the connections between Noah LSM and
762 ParFlow, and thus WRF.

763 In the presence of a vegetation layer, plant transpiration (length per unit time) is determined
764 as follows:

$$765 \quad T(x, z) = G(z)C_{plant}f_{veg}E_{pot}, \quad (25)$$

766 where $C_{plant}(-)$ represents a constant coefficient between 0 and 1, which depends on vegetation
767 species, and the $G(z)$ function represents soil moisture which provides other connection between
768 the coupled models (i.e. ParFlow, Noah, and WRF). The solution procedure of PF.WRF uses an
769 operator–splitting approach where both model components use the same time step. WRF soil
770 moisture information including runoff, surface ponding effects, unsaturated and saturated flow,
771 which includes an explicitly resolved water table are calculated and sent directly to the Noah LSM
772 within WRF by ParFlow and utilized by the Noah LSM in the next time step. WRF supplies
773 ParFlow with evapotranspiration rates and precipitation via the Noah LSM (Jiang et al., 2009).
774 The interdependence between energy and land balance of the subsurface, ground surface, and
775 lower atmosphere can fully be studied with this coupling approach. The coupled PF.WRF via the
776 Noah-LSM has been used to simulate explicit water storage and precipitation within basins, to
777 simulate surface runoffs and to simulate the land-atmosphere feedbacks and wind patterns as a
778 results of subsurface heterogeneity (Maxwell et al., 2011; Williams and Maxwell, 2011). Studies
779 with coupled model PF.WRF are highlighted in Table 2.

780 5.4 ParFlow–Advanced Regional Prediction System (PF. ARPS).

781 The Advanced Regional Prediction System (ARPS) composed of a parallel mesoscale
782 atmospheric model created to explicitly predict convective storms and weather systems. The ARPS
783 platform aids in effectively investigating the changes and predictability of storm-scale weather in
784 both idealized and more realistic settings. The model deals with the three dimensional, fully
785 compressible, non-hydrostatic, spatially filtered Navier-Stokes equations (Rihani et al., 2015). The
786 governing equations include conservation of momentum, mass, water, heat or thermodynamic,
787 turbulent kinetic energy, and the equation of state of moist air making use of a terrain-following
788 curvilinear coordinate system (Xue et al., 2000). The governing equations presented in a
789 coordinate system with z as the vertical coordinate are given as

$$790 \quad \frac{d\mathbf{v}}{dt} = -2\boldsymbol{\Omega} \times \mathbf{v} - \frac{1}{\rho} \nabla P + g + F \quad (26)$$

$$791 \quad \frac{d\rho}{dt} = -\rho \nabla \cdot \mathbf{v} \quad (27)$$

$$792 \quad \frac{dT}{dt} = -\frac{RT}{c_v} \nabla \cdot \mathbf{v} + \frac{Q}{c_v} \quad (28)$$

$$793 \quad P = \rho RT \quad (29)$$

794 Equations (26) to (29) are momentum, continuity, thermodynamic and equation of state,
795 respectively. The material (total) derivative d/dt is defined as

$$796 \quad \frac{d}{dt} = \frac{\partial}{\partial t} + \nabla \cdot \mathbf{v} \quad (30)$$

797 The variables \mathbf{v} , ρ , T , P , g , F , Q in equations (26) to (29) represent velocity [LT^{-1}], density
798 [ML^{-3}], temperature [K], pressure [$ML^{-1}T^{-2}$], gravity [LT^{-2}], frictional force [MLT^{-2}], and the

799 ~~diabatic heat source~~ [$\text{ML}^{-2}\text{T}^{-2}$], ~~density, temperature, pressure, gravity, frictional force, and the~~
800 ~~diabatic heat source~~, respectively (Xu et al., 1991). The ARPS model employs high-order
801 monotonic advection technique for scalar transport and fourth-order advection for other variables
802 e.g. mass density and mass mixing ratio. A split-explicit time advancement scheme is utilized with
803 leapfrog on the large time steps, and an explicit and implicit scheme for the smaller time steps is
804 used to inculcate the acoustic terms in the equations (Rihani et al., 2015).

805 The PF.ARPS forms a fully-coupled model that simulates spatial variations in above
806 ground processes and feedbacks, forced by physical processes in the atmosphere and the below the
807 ground surface. In the online coupling process, ARPS land surface model forms the interface
808 between ParFlow and ARPS to transmit information (i.e. surface moisture fluxes) between the
809 coupled models. ParFlow as a component of the coupled model replaces the subsurface hydrology
810 in the ARPS land surface model. Thus, ARPS is integrated into ParFlow as a subroutine to create
811 a numerical overlay at the coupling interphase (specified layers of soil within the land surface
812 model in ARPS) with the same number of soil layers at the ground surface within ParFlow. The
813 solution approach employed is an operator-splitting that allows ParFlow to match the ARPS
814 internal timesteps. ParFlow calculates the subsurface moisture field at each timestep of a
815 simulation and passes the information to ARPS land surface model, which is used in each
816 subsequent timestep. At the beginning of each time step, the surface fluxes from ARPS that are
817 important to ParFlow include evapotranspiration rate and spatially-variable precipitation
818 (Maxwell et al., 2007). PF. ARPS has been applied to investigate the effects of soil moisture

819 heterogeneity on atmospheric boundary layer processes. PF.ARPS keeps a realistic soil moisture
820 that is topographically-driven distribution and shows spatiotemporal relationship between water
821 depth, land surface and lower atmospheric variables (Maxwell et al., 2007; Rihani et al., 2015). A
822 summary of current studies involving PF. ARPS is included in Table 2.

823

824 5.5 ParFlow–CrunchFlow (ParCrunchFlow)

825 CrunchFlow is a software package developed to simulate multicomponent multi-
826 dimensional reactive flow and transport in porous and/or fluid media (Steefel, 2009). Systems of
827 chemical reactions that can be solved by the code include kinetically controlled homogenous and
828 heterogeneous mineral dissolution reactions, equilibrium–controlled homogeneous reactions,
829 thermodynamically controlled reactions, and biologically–mediated reactions (Steefel and Lasaga,
830 1994; Steefel and Yabusaki, 2000). In CrunchFlow, discretization of the governing coupled partial
831 differential equations which connect subsurface kinetic reactions and multicomponent
832 equilibrium, flow and solute transport is based on finite volume. (Li et al., 2007; Li et al., 2010).
833 Coupling of reactions and transport in CrunchFlow that are available at runtimes are performed
834 using two approaches. These are briefly discussed below.

835 First, a global implicit or one–step method approach is based on a backwards Euler time
836 discretization, with a global solution of the coupled reactive transport equations using Newton’s
837 method. This global implicit scheme solves the transport and reaction terms simultaneously (up to
838 two-dimensional) (Kirkner and Reeves, 1988; Steefel, 2009). Second, a time or operator splitting

839 of the reaction and transport terms which is based on an explicit forward Euler method; the
840 sequential non-iterative approach, SNIA (in which the transport and reaction terms are solved)
841 (Steeffel and Van Cappellen, 1990; Navarre-Sitchler et al., 2011). The stability criteria associated
842 with the explicit approach is that the simulation timestep is restricted via the Courant-Friedrichs-
843 Lewy (CFL) condition, under the circumstance that the transportation of mass does not occur over
844 multiple grid cells, but a single grid cell in a timestep. Thus, a small-time step must be used to
845 ensure this condition holds. This small step size may lead to simulations that will demand much
846 time to solve Beisman, (2007), so more processors are used, in order to decrease the processor
847 workload and decrease solution time of the simulation. Coupling of fully saturated flow to the
848 reactive transport calculations and coupling between a partially saturated flow and transport (flow
849 and diffusion) can be done successively. However, these simulations require calculations of the
850 flow and liquid saturation fields with a different model.

851 ParCrunchFlow is a parallel reactive transport model developed by combining ParFlow
852 with CrunchFlow. ParCrunchFlow was designed to be only applicable for subsurface simulation.
853 The coupled model ParCrunchFlow relies on ParFlow's robustness ability to efficiently represent
854 heterogeneous domains and simulate complex flow to provide a more realistic representation of
855 the interactions between biogeochemical processes and non-uniform flow fields in the subsurface
856 than the uncoupled model. ParFlow provides solution of Richards' equation to ParCrunchFlow,
857 which is not present in the biogeochemical code CrunchFlow. ParCrunchFlow employs operator-
858 splitting method to reactive transport, in which the transport and reaction terms are decoupled and
859 calculated independently. Online couplingCoupling between the models is achieved through a

860 sequential non-iterative approach, where the reaction terms in CrunchFlow’s operator-splitting
861 solver gets connected to ParFlow’s advection terms. ParCrunchFlow takes advantage of
862 multidimensional advection capability of ParFlow instead of CrunchFlow’s advective-dispersive
863 transport capabilities (up to two-dimensional). A steady state governing differential equation for
864 reaction and advection (with no dispersion and diffusion terms) in a single-phase system is given
865 by

$$866 \quad \frac{\partial C_i}{\partial t} + \nabla \cdot (\mathbf{V}v C_i) - R_i = 0, \quad (i = 1, N_{tot}) \quad (31)$$

867 where C_i is the concentration of species i , $\mathbf{V}v$ represents velocity of flow, R_i indicates total reaction
868 rate of species i , and N_{tot} represents total species number. In the coupling process, the advection
869 terms are calculated by ParFlow’s transport solver through a first-order explicit upwind scheme or
870 a second-order explicit Godunov scheme. Low-order upwind weighting schemes can introduce
871 numerical dispersion, which can impact the simulated reactions, and a comparison of several
872 upwinding schemes can be found in (Benson et al., 2017). CrunchFlow calculates the reaction
873 terms using the Newton-Raphson method. For example, in the coupled-model ParCrunchFlow,
874 ParFlow code assigns all hydrological parameters, undertakes the functions relating to
875 parallelization including domain decomposition and message transmission, and solves for pressure
876 and flow fields. The CrunchFlow module is then used to evaluate all reaction terms and
877 conversions between mobile and immobile concentrations. Sequence of simulations of a floodplain
878 aquifer, comprising biologically mediated reduction of nitrate have been performed with
879 ParCrunchFlow. The simulations demonstrate that ParCrunchFlow realistically represents the

880 changes in chemical concentrations seen in most field scale systems than CrunchFlow alone
881 (summarized in Table 2) (Beisman, 2007; Beisman et al., 2015).

882 Figure 5 Caption: Schematic of the communication structure of the coupled models. Note: CLM
883 represents a stand-alone Community Land Model. The modified version of CLM by Dai et al.,
884 (2003) is not shown here because it is a module only for ParFlow, not really a stand-alone LSM
885 any longer.

886

887 6. Discussion and Summary

888 IHMs constitute classes of simulation tools ranging from simple lumped parameter models
889 to comprehensive deterministic, distributed and physically based modeling systems for simulation
890 of multiple hydrological processes (LaBolle et al., 2003; Castronova et al., 2013). They are
891 indispensable in studying the interactions between surface and subsurface systems. IHMs that
892 calculate surface and subsurface flow equations in a single matrix (Maxwell et al., 2015), scaling
893 from the beginning parts to the mouth of continental river basins at high-resolutions are essential
894 (Wood, 2009) in understanding and modeling surface-subsurface systems. IHMs have been used
895 to address surface and subsurface science and applied questions. For example, evaluating the
896 effects of groundwater pumping on streamflow and groundwater resources (Markstrom et al.,
897 2008), evaluating relationship between topography and groundwater (Condon and Maxwell,
898 2015), coupling water flow and transport (Sudicky et al., 2008; Weill et al., 2011) and assessing

899 the resilience of water resources to human stressors or interventions and the variations in the
900 (Maxwell et al., 2015) over large spatial extents at high resolution. Modeling or simulation at large
901 spatial extents e.g. regional and continental scales and resolution e.g. 1km^2 (see Figure 6), and
902 even small spatial scale (Figure 7) comes with the associated computational load even on
903 massively parallel computing architectures. IHMs, such as ParFlow have overcome the
904 computational burden of simulating or resolving questions (e.g. involving approximating variably
905 saturated and overland flow equations) beyond such levels of higher spatial scales and resolutions.
906 This capability may not be associated with more conceptually based models which, for example,
907 may not simulate lateral groundwater flow or resolve surface and subsurface flow by specifying
908 zones of groundwater network of stream before performing a simulation (Maxwell et al., 2015)
909 For cross-comparison of ParFlow with other contemporary IHMs, a more comprehensive model
910 testing and analyses have recently been done and readers can access these resources at Maxwell et
911 al., (2014), Koch et al., (2016) and Kollet et al., (2017).

912 Figure 6 Caption: Map of water table depth (m) over the simulation domain with two insets
913 zooming into the North and South Platte River basin, headwaters to the Mississippi River. Colors
914 represent depth in log scale (from 0.01 to 100 m) (Maxwell et al., 2015).

915 Figure 7 Caption: Map of hydraulic conductivity (K) and stream depth in the East Inlet watershed
916 in Colorado (Engdahl and Maxwell, 2015). This domain covers 30km^2 using 3.1 million 20m^2
917 (lateral grid cells. The springs emanating from within the hillslopes highlight the realism afforded
918 by integrated modeling at small scales.

919
920
921
922
923
924
925
926
927
928
929
930
931
932
933
934
935
936
937
938
939

ParFlow is based on efficient parallelism (high performance efficiency) and robust hydrologic capabilities. The model solvers and numerical methods used are powerful, fast, robust, and stable, which has contributed to the code's excellent parallel efficiency. As stated earlier, ParFlow is very capable of simulating flows under saturated and variably saturated conditions i.e. surface, vadose, and groundwater flows, even in highly heterogeneous environments. For example, in simulation of surface flows (i.e. solving the kinematic wave overland flow equations), ParFlow possess the ability to accurately solve streamflow (channelized flow) by using parameterized river routing subroutines (Maxwell and Miller, 2005; Maxwell et al., 2007, 2011). ParFlow includes coupling capabilities with a flexible coupling interface which has been utilized extensively in resolving many hydrologic problems. The interface-based and process-level coupling used by ParFlow is an example for enabling high-resolution, realistic modeling. However, based on the applications, it would be worthwhile to create one, or several, generic coupling interfaces within ParFlow to make it easier to use its surface/subsurface capabilities in other simulations. Nonetheless, ParFlow has been used in coupling studies in simulating different processes and/or systems including simulating energy and water budgets of the surface and subsurface (Rihani et al., 2010; Mikkelsen et al., 2013), surface water and groundwater flows and transport (Kollet and Maxwell, 2006; Beisman, 2007; Beisman et al., 2015; Maxwell et al., 2015), and subsurface, surface, and atmospheric mass and energy balance (Maxwell and Miller, 2005; Maxwell et al., 2011; Shrestha et al., 2014; Sulis et al., 2017). Undoubtedly, such coupled-model simulations come with computational burden and ParFlow performs well in overcoming such problems, even at high

940 spatial scale and resolutions. This capability of ParFlow (coupling with other models) is
941 continuously being exploited by hydrologic modelers, and new couplings are consistently being
942 established. For example, via model coupling, the entire transpiration process could be investigated
943 i.e. from carbon dioxide sequestration from the atmosphere by plants, subsurface moisture
944 dynamics and impacts, to oxygen production by plants. Likewise, land cover change effects on
945 mountain pine beetles may be investigated via coupling of integrated models. But these projected
946 research advances can only be achieved if the scientific community keeps advancing code
947 performance by developing, revising, updating, and rigorously testing these models' capabilities.

948 Presently, ParFlow's open source model and open developer community is fully
949 transparent, and this openness is a major difference between it and other models that has enabled
950 ParFlow to continue evolving. The user community is growing daily across the globe. Code
951 developers have made available, aside from the ParFlow working manual, an active and
952 frequently-updated blog (current blog: "<http://parflow.blogspot.com/>") and other sources
953 including "<https://www.parflow.org>" and "<https://github.com/parflow>" where code developers and
954 experienced users provide great information and suggestions that help in fixing bugs and ease
955 frustrations of other users. Over the years, these easily accessible resources have proven to be
956 helpful. The code is constantly updated through release of new versions with modifications
957 designed to meet varying hydrologic challenges and directions for applications across different
958 scales and fields. Each ParFlow package (version) comes with verified simulation test cases with
959 directions that simulate different real systems and idealized cases. These serve as great resource
960 where additional code modifications have been tested in every release of the code. ParFlow has a

961 clear, rigorous verification procedure to make sure that any changes checked in do not “break”
962 previous developments. This ensures numerical accuracy and backwards compatibility. Moreover,
963 the full suite of test cases is automatically re-run before any submitted change can even be
964 considered for merging with the master branch of the code. The number of branches/forks cannot
965 be controlled in any open source (or community) code, but any contributions to the master branch
966 are exhaustively vetted before being pushed out to users. Further, there is a software development
967 and sustainability plan to improve the capabilities of ParFlow such as incorporation of new
968 formulations of both kinematic and diffusive wave approximations, and advanced parallelization
969 support (GPU’s and heterogeneous compute architectures). ParFlow works very well on different
970 computing architectures and operating systems from “Laptops to Supercomputers” (single CPU,
971 Linux clusters, highly scalable systems including IBM Blue Gene) with the same source code and
972 input on all platforms. The code can use significant computational power and runs efficiently on
973 supercomputing environments (e.g. Edison, Cori, JUQUEEN, and Yellowstone). Through
974 ParFlow hydrologic modelers have available a very efficient yet still growing integrated
975 hydrologic model to simulate and understand surface-subsurface flows.

976 Code availability

977 ParFlow is an open–source, object–oriented, parallel watershed flow model developed by
978 community of scientists from the Environmental Protection Department at the Lawrence
979 Livermore National Laboratory (LLNL), Colorado School of Mines and F-Z Jülich with
980 supporting scientists from several other institutions. ~~Versions of ParFlow are archived with~~
981 ~~detailed document or information located at:~~
982 ~~http://inside.mines.edu/~rmaxwell/maxwell_software.shtml or obtain from commercially hosted~~
983 ~~free SVN repository. Source code for the current ParFlow release “v3.5.0” can be downloaded at:~~
984 ~~<https://github.com/parflow/parflow/releases/tag/v3.5.0>.~~ The current version of ParFlow is

985 [available at: https://github.com/parflow/parflow/releases/tag/v3.6.0](https://github.com/parflow/parflow/releases/tag/v3.6.0). The version of ParFlow
986 [described in this manuscript is archived on zenodo: https://doi.org/10.5281/zenodo.3555297](https://doi.org/10.5281/zenodo.3555297).

987 Author Contribution

988 Section 3 of the manuscript was written by Carol S. Woodward. Benjamin N. O. Kuffour and
989 Nicholas B. Engdahl wrote the other Sections, and the entire manuscript was edited by Laura E.
990 Condon, Stefan Kollet, and Reed M. Maxwell.

991 Competing Interest

992 We declare that no conflict of interest exist whatsoever between any of the authors and the editors
993 or the referees.

994 Acknowledgement

995 We kindly acknowledge funding of the project by the U.S. Department of Energy, Office of
996 Science (Subsurface Biogeochemical Research), Award number DE-SC0019123.

997

998

999

1000

1001

1002

1003

1004

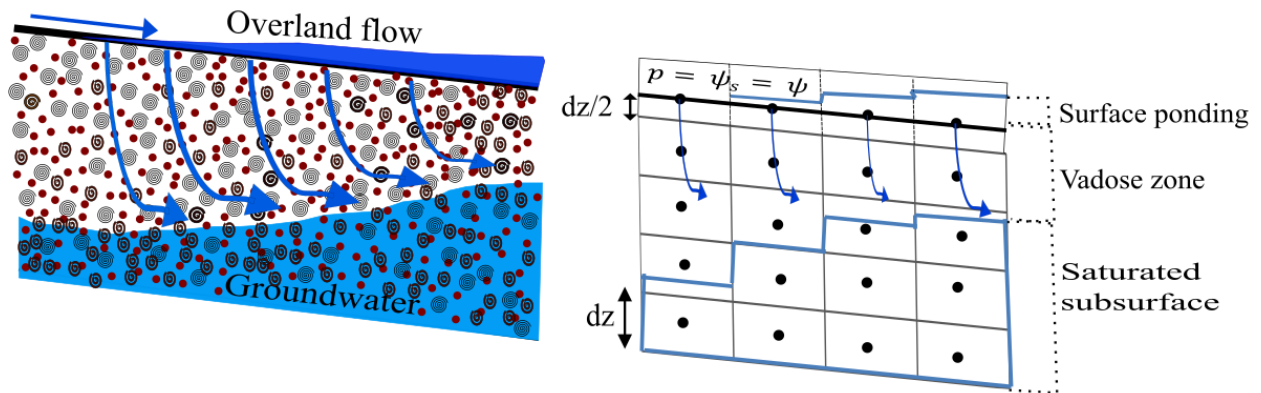
1005

1006

1007

1008

FIGURES



1009

1010 Figure 1: Coupled surface and subsurface flow systems. The physical system is represented on the

1011 left and a schematic of the overland flow boundary condition (continuity of pressure and flux at

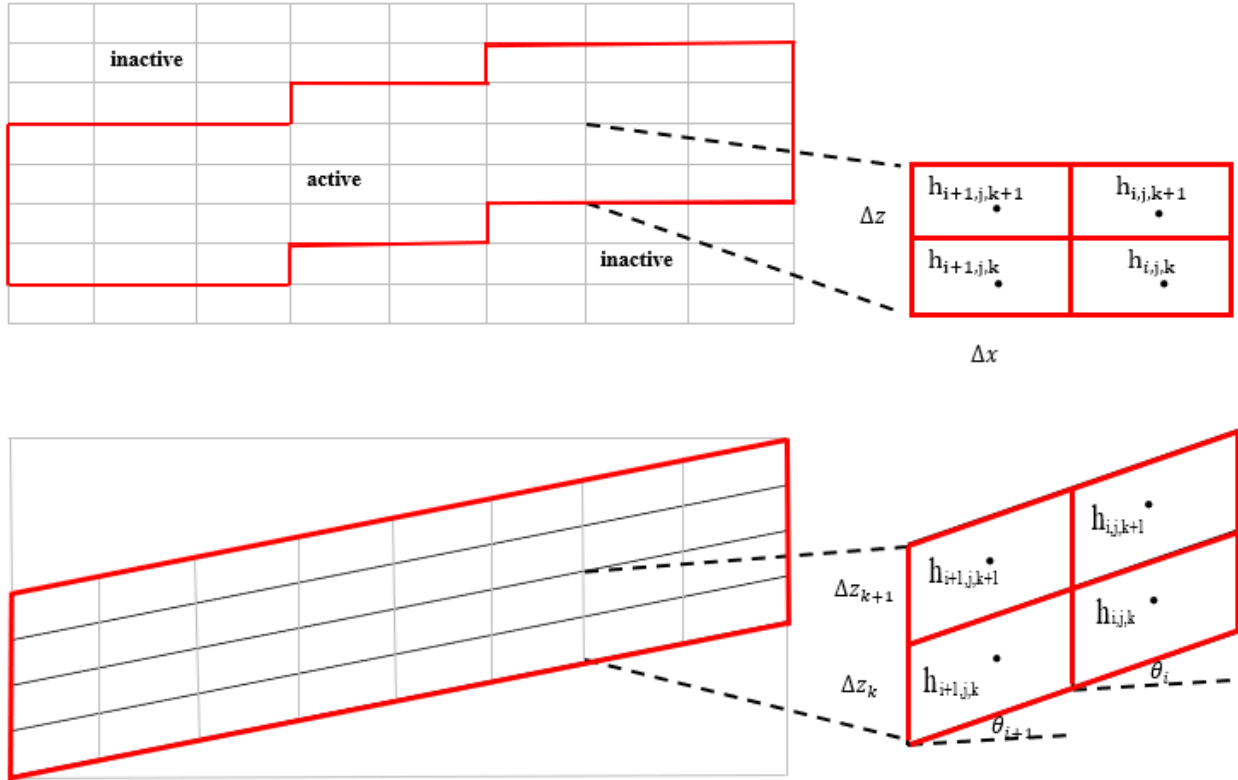
1012 the ground surface) is on the right. The equation, $p = \psi_s = \psi$ in Figure 1 signifies that at the

1013 ground surface, the vertically averaged surface pressure and subsurface pressure head are equal,

1014 which is the unique overland flow boundary used by ParFlow.

1015

1016



1017

1018 Figure 2: Representation of orthogonal (upper) and the terrain following (lower) grid formulations
 1019 and schematics of the associated finite difference dependences (right). The i , j , and k are the x , y ,
 1020 and z cell indices

1021

1022

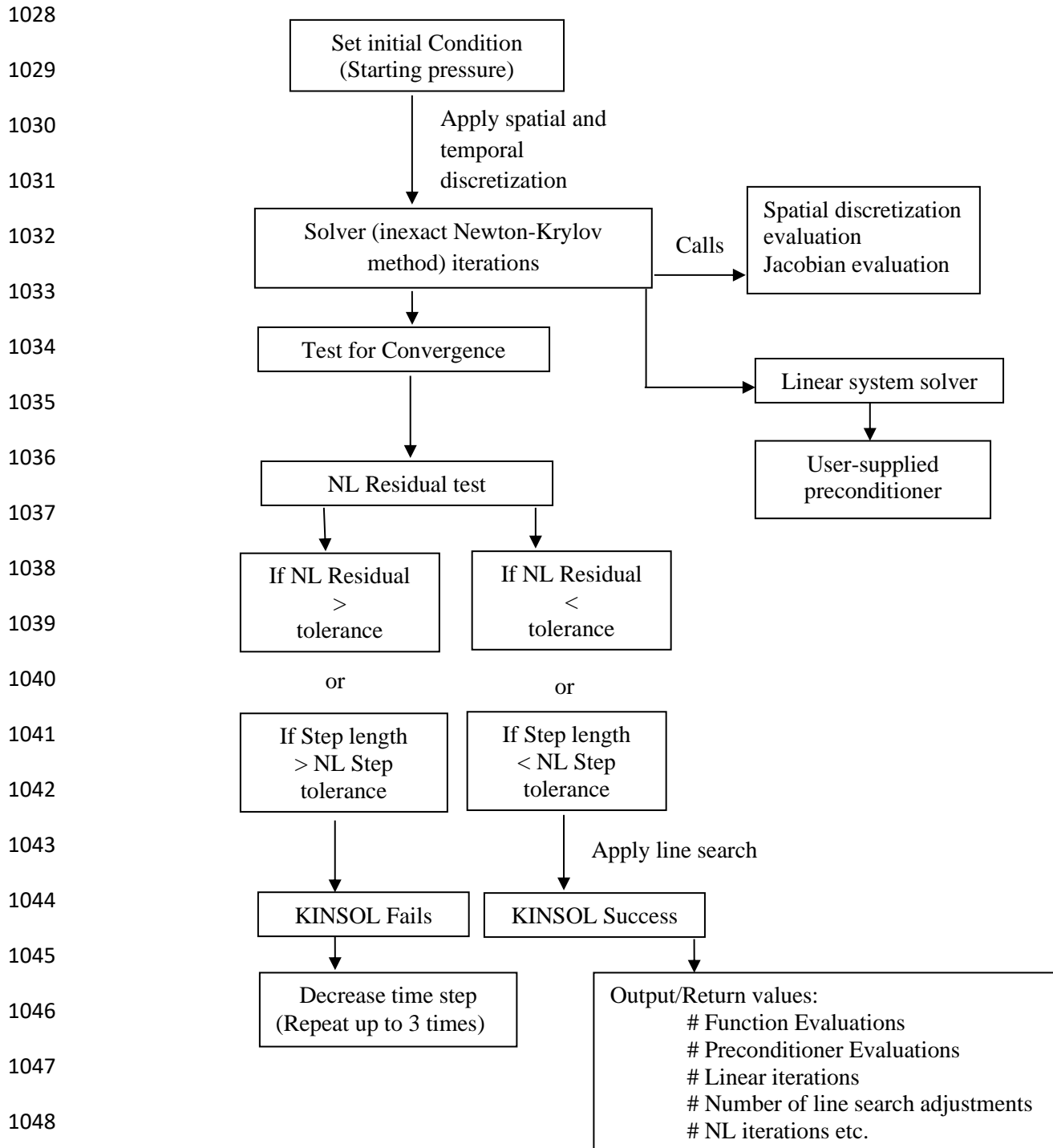
1023

1024

1025

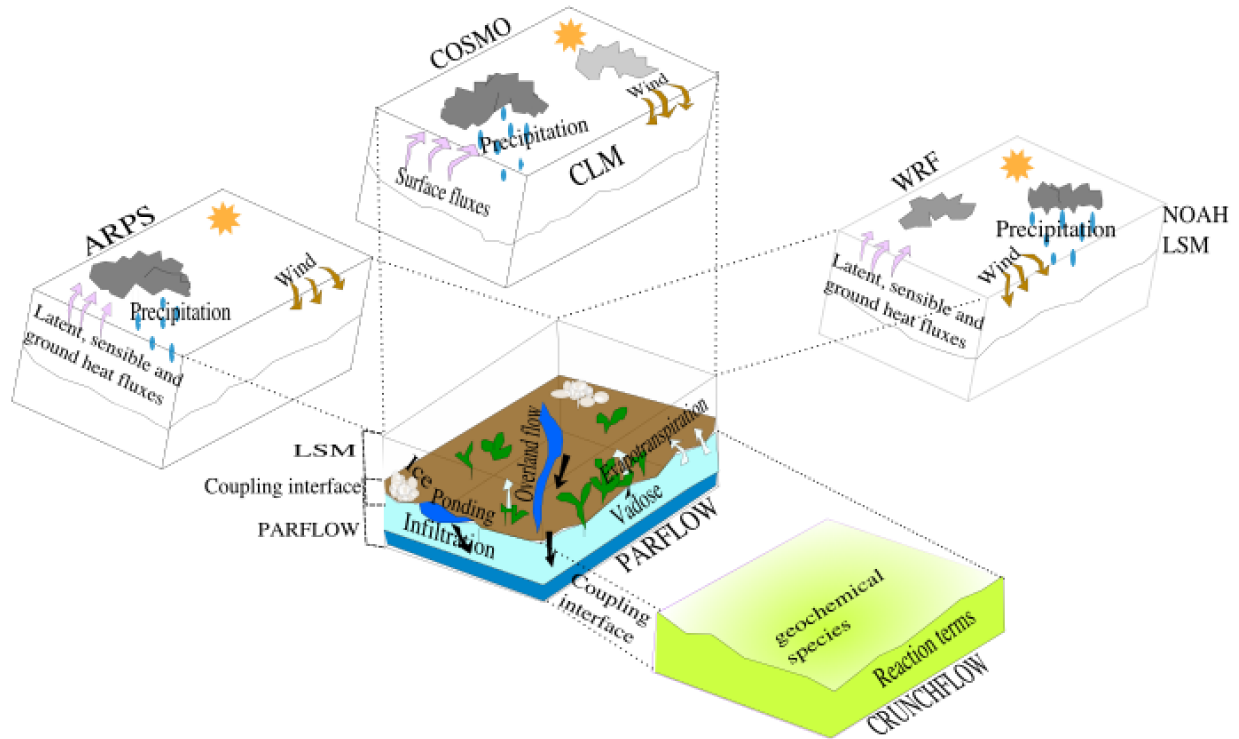
1026

1027



1049 Figure 3: Working flow chart of ParFlow's solver for linear and non-linear system solution

1050



1051

1052 Figure 4(a): A pictorial description of the relevant physical environmental features and model

1053 coupling. CLM represents the Community Land Model, a stand-alone Land Surface Model (LSM)

1054 via which ParFlow couples' COSMO. The modified version of CLM by Dai et al., (2003) and is

1055 not shown in Figure 4(a) because it is a module only for ParFlow, not really a stand-alone LSM

1056 any longer. The core model (ParFlow) always solves the variably saturated 3-D groundwater flow

1057 problem but the various couplings add additional capabilities.

1058

1059

1060

1061

1062
1063
1064
1065
1066
1067
1068
1069
1070
1071
1072
1073
1074
1075
1076
1077
1078
1079
1080
1081
1082
1083

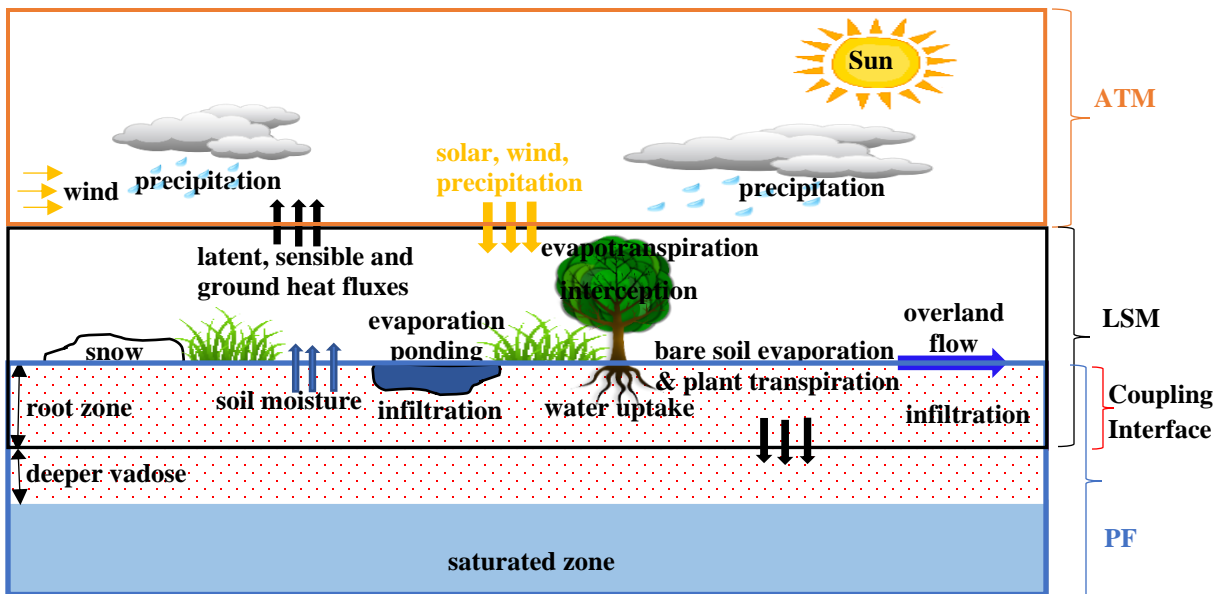


Figure 4(b): Schematic showing information transmission at the coupling interface. PF, LSM, and ATM indicate the portions of the physical system simulated by ParFlow, Land Surface Models, and Atmospheric Models respectively. The downward and upward arrows indicate the directions of information transmission between adjacent models. Note: Coupling between ParFlow and CrunchFlow (not shown) occur within the subsurface.

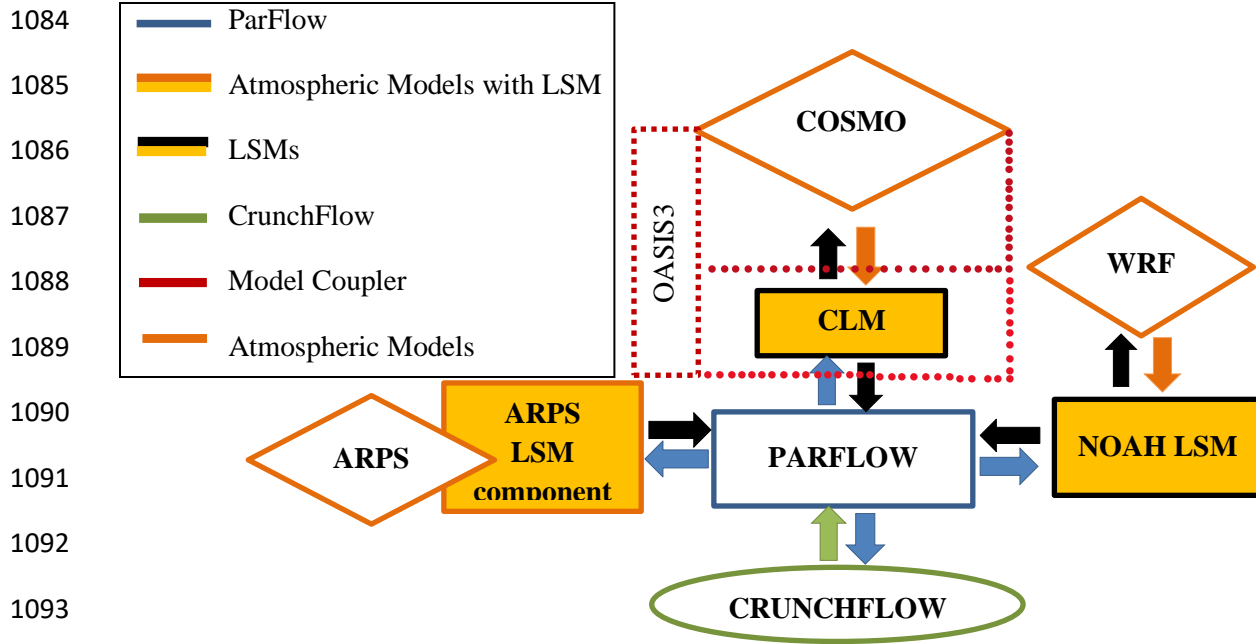


Figure 5: Schematic of the communication structure of the coupled models. Note: CLM represents a stand-alone Community Land Model. The modified version of Common Land Model by Dai et al., (2003) is not shown here because it is a module only for ParFlow, not really a stand-alone LSM any longer.

1094

1095

1096

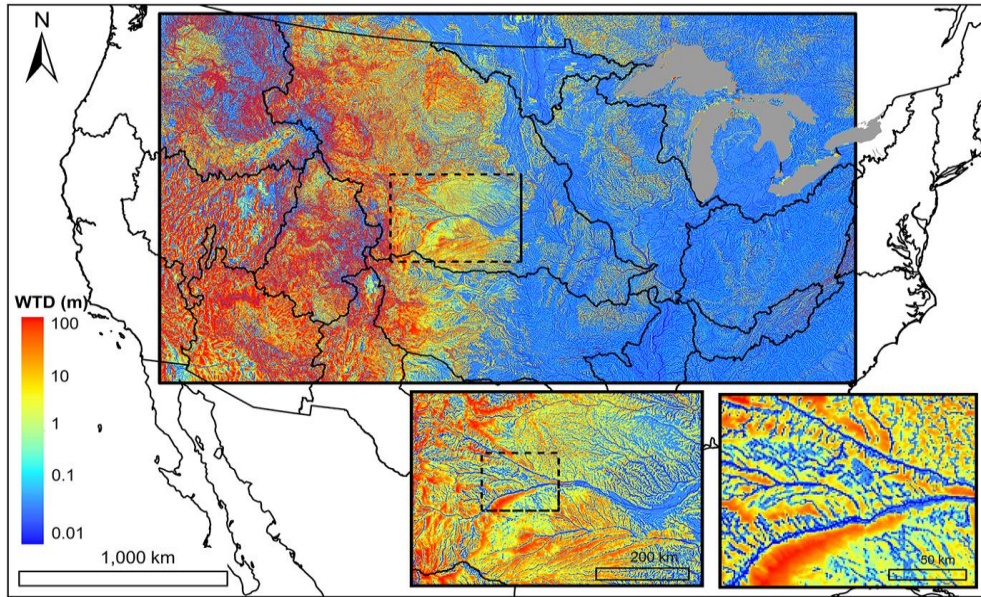
1097

1098

1099

1100

1101



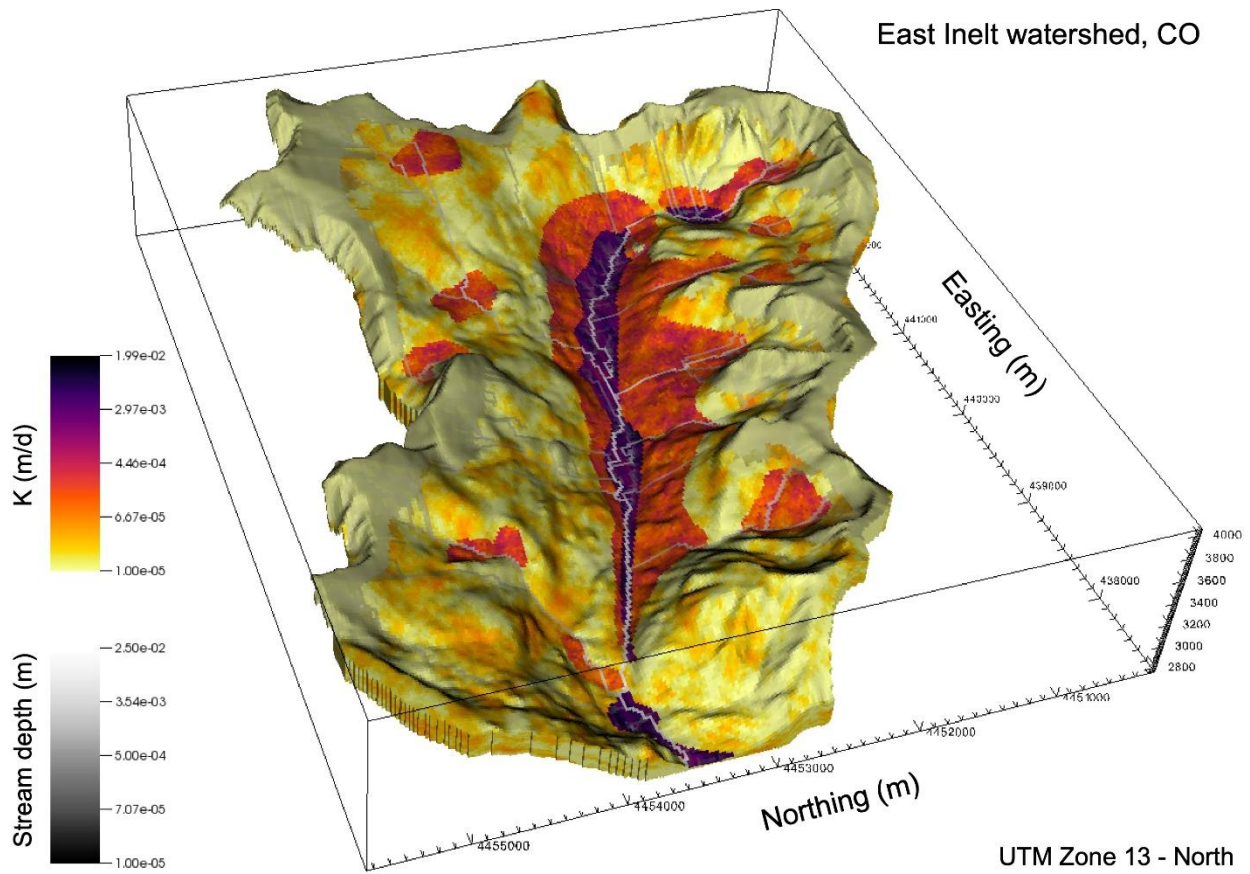
1102

1103 Figure 6: Map of water table depth (m) over the simulation domain with two insets zooming into
1104 the North and South Platte River basin, headwaters to the Mississippi River. Colors represent depth
1105 in log scale (from 0.01 to 100 m) (reproduced from Maxwell et al., 2015). The domain uses 1km^2
1106 grid cells and represents one of the largest, and highest resolution domains simulated by integrated
1107 models to date.

1108

1109

1110



1111

1112

1113 Figure 7: Map of hydraulic conductivity (K) and stream depth in the East Inlet watershed in
 1114 Colorado (Engdahl and Maxwell, 2015). This domain covers 30km² using 3.1 million 20m² lateral
 1115 grid cells. The springs emanating from within the hillslopes highlight the realism afforded by
 1116 integrated modeling at small scales.

1117

1118

1119

1120 Table 1: Details for the various scaling studies conducted using ParFlow

Simulation Case	Computer System	Processor Number	Jacobian/ Numerical Method	Preconditioner	Computation time (seconds)	Problem Size (cell Number)	Parallel Efficiency (%)	Study
Surface processes and variably saturated flow (ParFlow and CLM)	JUGENE (IBM Blue-Gene Super-computer)	16,384	Finite difference	ParFlow Multigrid	10,920	486,000	58.00	(Kollet et al., 2010)
Terrain Following Grid	JUGENE (IBM Blue-Gene Super-computer)	4,096	Analytical	Non-Symmetric	1,130.50	2,048,000,000	80.91	(Maxwell, 2013)
Overland flow	Intel Xeon Tightly coupled Linux Cluster	100	Finite difference	–	10,800	50,000	82.00	(Kollet and Maxwell, 2006)
Excess infiltration produced runoff	Intel Xeon Tightly coupled Linux Cluster	100	Finite difference	–	10,800	50,000	72.00	(Kollet and Maxwell, 2006)
Terrain Following Grid	JUGENE (IBM Blue-Gene Super-computer)	16,384	Finite difference	Symmetric	2,100.81	8,192,000,000	50.60	(Maxwell, 2013)
Subsurface and Overland flow coupling	IBM BGQ architecture	1,024	Analytical /Finite difference	ParFlow Multigrid	7,200	150,000	50.00	(Osei-Kuffuor et al., 2014)
Fully coupling terrestrial systems modeling platform	IBM BGQ system JUQUEEN	4,096	–	–	–	38,880	82.00	(Gasper et al., 2014)
Performance evaluation of ParFlow code (modified version of ParFlow)	(IBM Blue-Gene Super-computer) JUQUEEN	458,752	Finite difference	–	–	10,569,646,080	–	(Burstedde et al., 2018)

1121 Note: The hyphen “–” shows that information was not provided by the appropriate study

1122

1123 Table 2: Selected coupling studies involving application of ParFlow and atmospheric, land surface, and subsurface models

Application	Coupled Model	Simulation Scale	Study
Surface heterogeneity, surface energy budget	CLM	Urban watershed Ballona Creek watershed, CA	(Reyes et al., 2016)
Sensitivity analysis (evaporation parameterization)	CLM (modified)	Column	(Jefferson and Maxwell, 2015)
Sensitivity of photosynthesis and stomatal resistivity parameters	CLM (modified)	Column	(Jefferson et al., 2017)
Active subspaces; dimension reduction; energy fluxes	CLM (modified)	Hillslope	(Jefferson et al., 2015)
Spin-up behavior; initial conditions watershed	CLM	Regional	(Seck et al., 2015)
Urban processes	CLM	Regional	(Bhaskar et al., 2015)
Global sensitivity	CLM	watershed	(Srivastava et al., 2014)
Entropy production optimization and inference principles	CLM	Hillslope	(Kollet, 2015)
Soil moisture dynamics	CLM	Catchment	(Fang et al., 2015)
Dual boundary forcing concept	CLM	Catchment	(Rahman et al., 2015)
Initial conditions; Spin-up	CLM	Catchment; Watershed	(Ajami et al., 2014, 2015)
Groundwater fed irrigation impacts of natural systems; optimization water allocation algorithm	CLM	Watershed; Sub-watershed	(Condon and Maxwell, 2013, 2014)
Subsurface heterogeneity (land surface fluxes)	CLM	Watershed	(Condon et al., 2013)
Mountain Pine Beetle	CLM	Hillslope	(Mikkelsen et al., 2013)
Groundwater land surface-atmosphere feedbacks	CLM	Watershed	(Ferguson and Maxwell, 2010, 2011, 2012)
Subsurface heterogeneity (land surface processes)	CLM	Hillslope	(Atchley and Maxwell, 2011)
Computational scaling	CLM	Hillslope	(Kollet et al., 2010)
Subsurface heterogeneity (infiltration in arid environment)	CLM	Hillslope	(Maxwell, 2010)
Subsurface heterogeneity (land energy fluxes)	CLM	Hillslope	(Rihani et al., 2010)
Heat and subsurface energy transport (ParFlowE)	CLM	Column	(Kollet et al., 2009)
Subsurface heterogeneity on evapotranspiration	CLM	Column, Hillslope	(Kollet, 2009)
Subsurface heterogeneity (land energy fluxes; runoff)	CLM	Watershed; Hillslope	(Kollet and Maxwell, 2008)
Climate change (land energy feedbacks to groundwater)	CLM	Watershed	(Maxwell and Kollet, 2008)
Model development	CLM	Column	(Maxwell and Miller, 2005)
Subsurface transport	CLM	Aquifer	(Tompson et al., 1998, 1999; Maxwell et al., 2003)
Model development (TerrSysMP)	COSMO	Watershed	(Shrestha et al., 2014)
Implementation and Scaling (TerrSysMP)	COSMO	Continental	(Gasper et al., 2014)

Groundwater response to ground surface-atmosphere feedbacks	COSMO	European CORDEX domain (Continental)	(Keune et al., 2016)
Atmosphere, DART, data assimilation	WRF	Watershed	(Williams et al., 2013)
Coupled model development (Atmosphere)	WRF	Watershed	(Maxwell et al., 2011)
Subsurface heterogeneity (runoff generation)	WRF	Hillslope	(Meyerhoff and Maxwell, 2010)
Subsurface uncertainty to the atmosphere	WRF	Watershed	(Williams and Maxwell, 2011)
Subsurface transport	ARPS	Watershed	(Maxwell et al., 2007)
Terrain and soil moisture heterogeneity on atmosphere	ARPS	Hillslope	(Rihani et al., 2015)
Risk Assessment of CO leakage	CRUNCHFLOW	Aquifer	(Atchley et al., 2013)
Reactive transport heterogeneous saturated subsurface environment	CRUNCHFLOW	Aquifer	(Beisman et al., 2015)

1124 Note: "CLM" show that coupling with ParFlow was by the original Common Land Model or Community Land Model. "CLM (modified)" show that the
1125 modified version of Common Land Model by (Dai et al., 2003) was a module for ParFlow.

<u>Application</u>	<u>Coupled Model</u>	<u>Simulation Scale and Size (x, y, and z dimensions)</u>	<u>Model Development</u>	<u>Model Calibration</u>	<u>Study</u>
<u>Surface heterogeneity, surface energy budget</u>	<u>CLM</u>	<u>Watershed (30m x 30m x 84m)</u>			<u>(Reyes et al., 2016)</u>
<u>Sensitivity analysis (evaporation parameterization)</u>	<u>CLM (modified)</u>	<u>Column (1m x 1m x 10m)</u>			<u>(Jefferson and Maxwell, 2015)</u>
<u>Sensitivity of photosynthesis and stomatal resistivity parameters</u>	<u>CLM (modified)</u>	<u>Column (2m x 2m x 10m)</u>			<u>(Jefferson et al., 2017)</u>
<u>Active subspaces; dimension reduction; energy fluxes</u>	<u>CLM (modified)</u>	<u>Hillslope (300m x 300m x 10m)</u>			<u>(Jefferson et al., 2015)</u>
<u>Spin-up behavior; initial conditions watershed</u>	<u>CLM</u>	<u>Regional (75km x 75km x 200m)</u>			<u>(Seck et al., 2015)</u>
<u>Urban processes</u>	<u>CLM</u>	<u>Regional (500m x 500m x 5m)</u>		<u>Yes</u>	<u>(Bhaskar et al., 2015)</u>
<u>Global sensitivity</u>	<u>CLM</u>	<u>Watershed (84km x 75km x 144m)</u>		<u>Yes</u>	<u>(Srivastava et al., 2014)</u>
<u>Entropy production optimization and inference principles</u>	<u>CLM</u>	<u>Hillslope (100m x 100m x 5m)</u>			<u>(Kollet, 2015)</u>
<u>Soil moisture dynamics</u>	<u>CLM</u>	<u>Catchment (1180m x 74m x 1.6m)</u>		<u>Yes</u>	<u>(Zhufeng et al., 2015)</u>
<u>Dual-boundary forcing concept</u>	<u>CLM</u>	<u>Catchment (49km x 49km x 50m)</u>			<u>(Rahman et al., 2015)</u>
<u>Initial conditions; Spin-up</u>	<u>CLM</u>	<u>Catchment; Watershed (28km x 20km x 400m)</u>			<u>(Ajami et al., 2014, 2015)</u>

Groundwater-fed irrigation impacts of natural systems; optimization water allocation algorithm	CLM	Watershed; Sub-watershed (41km x 41km x 100m)		(Condon and Maxwell, 2013, 2014)
Subsurface heterogeneity (land surface fluxes)	CLM	Watershed (209km x 268km x 3502m)		(Condon et al., 2013)
Mountain Pine Beetle	CLM	Hillslope (500m x 1000m x 12.5m)		(Mikkelsen et al., 2013)
Groundwater-land surface-atmosphere feedbacks	CLM	Watershed (32km x 45km x 128m)		(Ferguson and Maxwell, 2010, 2011, 2012)
Subsurface heterogeneity (land surface processes)	CLM	Hillslope (250m x 250m x 4.5m)		(Atchley and Maxwell, 2011)
Computational scaling	CLM	Hillslope (150m x 150m x 240m)		(Kollet et al., 2010)
Subsurface heterogeneity (infiltration in arid environment)	CLM	Hillslope (32km x 45km x 128m)		(Maxwell, 2010)
Subsurface heterogeneity (land energy fluxes)	CLM	Hillslope (5km x 0.1km x 310m)		(Rihani et al., 2010)
Heat and subsurface energy transport (ParFlowE)	CLM	Column (1m x 1m x 10m)	Yes	(Kollet et al., 2009)
Subsurface heterogeneity on evapotranspiration	CLM	Column, Hillslope (32m x 45m x 128m)		(Kollet, 2009)
Subsurface heterogeneity (land-energy fluxes; runoff)	CLM	Watershed; Hillslope (3km x 3km x 30m)		(Kollet and Maxwell, 2008)
Climate change (land-energy feedbacks to groundwater)	CLM	Watershed (3000m x 3000m x 30m)		(Maxwell and Kollet, 2008)
Model development experiment	CLM	Column	Yes	(Maxwell and Miller, 2005)
Subsurface transport	CLM	Aquifer (30m x 15m x 0.6m)		(Tompson et al., 1998, 1999; Maxwell et al., 2003)
Model development (TerrSysMP)	COSMO	Watershed (64km x 64km x 30m)	Yes	(Shrestha et al., 2014)
Implementation and Scaling (TerrSysMP)	COSMO	Continental	Yes	(Gasper et al., 2014)
Groundwater response to ground surface-atmosphere feedbacks	COSMO	Continental (436m x 424m x 103m)	Yes	(Keune et al., 2016)
Atmosphere, DART, data assimilation	WRF	Watershed (15km x 15km x 5m)	Yes	(Williams et al., 2013)
Coupled model development (Atmosphere)	WRF	Watershed (15km x 15km x 5m)	Yes	(Maxwell et al., 2011)

<u>Subsurface heterogeneity (runoff generation)</u>	<u>WRF</u>	<u>Hillslope (3km x 3km x 30m)</u>		<u>(Meyerhoff and Maxwell, 2010)</u>
<u>Subsurface uncertainty to the atmosphere</u>	<u>WRF</u>	<u>Watershed (15km x 15km x 5m)</u>	<u>Yes</u>	<u>(Williams and Maxwell, 2011)</u>
<u>Subsurface transport</u>	<u>ARPS</u>	<u>Watershed (17m x 10.2m x 3.8m)</u>	<u>Yes</u>	<u>(Maxwell et al., 2007)</u>
<u>Terrain and soil moisture heterogeneity on atmosphere</u>	<u>ARPS</u>	<u>Hillslope (5km x 2.5km x 80m)</u>		<u>(Rihani et al., 2015)</u>
<u>Risk Assessment of CO leakage</u>	<u>CRUNCHFLOW</u>	<u>Aquifer (84km x 75km x 144m)</u>	<u>Yes</u>	<u>(Atchley et al., 2013)</u>
<u>Reactive transport heterogeneous saturated subsurface environment</u>	<u>CRUNCHFLOW</u>	<u>Aquifer (120m x 120m x 120m)</u>		<u>(Beisman et al., 2015)</u>

1126 Note: "CLM" show that coupling with ParFlow was by the original Common Land Model or Community Land Model. "CLM (modified)" show that the
1127 modified version of Common Land Model by (Dai et al., 2003) was a module for ParFlow.

1128 References

- 1129 Abu-El-Sha’r, W. Y., and Rihani, J. F.: Application of the high performance computing
1130 techniques of parflow simulator to model groundwater flow at Azraq basin, *Water Resour.*
1131 *Manag.*, 21(2), 409–425, doi:10.1007/s11269-006-9023-5, 2007.
- 1132 Ajami, H., M. F. McCabe, Evans, J. P., and Stisen, S.: Assessing the impact of model spin-up on
1133 surface water-groundwater interactions using an integrated hydrologic model, *Water*
1134 *Resour. Res.*, 50, 1–21, doi:10.1002/2013WR014258.Received, 2014.
- 1135 Ajami, H., McCabe, M. F., and Evans, J. P.: Impacts of model initialization on an integrated
1136 surface water-groundwater model, *Hydrol. Process.*, 29(17), 3790–3801,
1137 doi:10.1002/hyp.10478, 2015.
- 1138 Allievi, A., and Calisal, S. M.: Application of Bubnov-Galerkin formulation to orthogonal grid
1139 generation, *J. Comput. Phys.*, 98(1), 163–173, doi:10.1016/0021-9991(92)90181-W, 1992.
- 1140 Amdahl, G. M.: Validity of the single processor approach to achieving large scale computing
1141 capabilities, in *spring joint computer conference*, vol. 37, 256–9, 1967.
- 1142 Anyah, R. O., Weaver, C. P., Miguez-Macho, G., Fan, Y., and Robock, A.: Incorporating water
1143 table dynamics in climate modeling: 3. Simulated groundwater influence on coupled land-
1144 atmosphere variability, *J. Geophys. Res. Atmos.*, 113(7), 1–15, doi:10.1029/2007JD009087,
1145 2008.
- 1146 Ashby, S. F., and Falgout, R. D.: A Parallel Multigrid Preconditioned Conjugate Gradient
1147 Algorithm for Groundwater Flow Simulations, *Nucl. Sci. Eng.*, 124, 145–159, 1996.
- 1148 Ashby, S. F., Falgout, R. D., Smith, S. G., and Tompson, A. F. B.: Modeling groundwater flow
1149 on MPPs, *Proc. Scalable Parallel Libr. Conf.*, 17–25, doi:10.1109/SPLC.1993.365586,
1150 1993.
- 1151 Ashby, S. F., Falgout, R. D., Tompson, A., and Fogwell, T.: Numerical simulation of
1152 groundwater flow on MPPs, , 17–25, 1994.
- 1153 Ashby, S. F., Falgout, R. D., and Tompson, A. F. B.: A Scalable Approach to Modeling
1154 Groundwater Flow on Massively Parallel Computers, in *In Next Generation Environmental*
1155 *Models and Computational Methods*, vol. 87, 201, 1997.
- 1156 Atchley, A. L., and Maxwell, R. M.: Influences of subsurface heterogeneity and vegetation cover
1157 on soil moisture, surface temperature and evapotranspiration at hillslope scales, *Hydrogeol.*
1158 *J.*, 19(2), 289–305, doi:10.1007/s10040-010-0690-1, 2011.
- 1159 Atchley, A. L., Maxwell, R. M., and Navarre-Sitchler, A. K.: Human health risk assessment of
1160 CO₂ leakage into overlying aquifers using a stochastic, geochemical reactive transport
1161 approach, *Environ. Sci. Technol.*, 47(11), 5954–5962, doi:10.1021/es400316c, 2013.
- 1162 Baldauf, M., Seifert, A., Forstner, J., Majewski, D., and Raschendorfer, M.: Operational
1163 Convective-Scale Numerical Weather Prediction with the COSMO Model : Description and
1164 Sensitivities, *Am. Meteorol. Soc.*, 3887–3905, doi:10.1175/MWR-D-10-05013.1, 2011.
- 1165 Beisman, J.: Development of a parallel reactive transport model with spatially variable nitrate
1166 reduction in a floodplain aquifer, 2007.
- 1167 Beisman, J. J., Maxwell, R. M., Steefel, C. I., and Molins, S.: ParCrunchFlow : an efficient ,
1168 parallel reactive transport simulation tool for physically and chemically heterogeneous
1169 saturated subsurface environments, 403–422, doi:10.1007/s10596-015-9475-x, 2015a.
- 1170 Beisman, J. J., Maxwell, R. M., Navarre-Sitchler, A. K., Steefel, C. I., and Molins, S.:
1171 ParCrunchFlow: an efficient, parallel reactive transport simulation tool for physically and
1172 chemically heterogeneous saturated subsurface environments, *Comput. Geosci.*, 19(2), 403–

1173 422, doi:10.1007/s10596-015-9475-x, 2015b.

1174 Bell, J. B., Dawson, C. N., and Shubin, G. R.: An unsplit, higher order godunov method for
1175 scalar conservation laws in multiple dimensions, *J. Comput. Phys.*, 74(1), 1–24,
1176 doi:10.1016/0021-9991(88)90065-4, 1988.

1177 Benson, D. A., Aquino, T., Bolster, D. N. E. C, and Christopher, D. F.G., Henri, V.: A
1178 comparison of Eulerian and Lagrangian transport and non-linear reaction algorithms, *Adv.*
1179 *Water Resour.*, 99, 15–37, 2017.

1180 Bettems, J. M., Asensio, H., Bonafe, Duniec, G., Fuhrer, O., Helmert, J., Heret, C., Kazakova,
1181 E., Lange, Machulskaya, E., Mazur, A., De Morsier, G., Rianna, G., Rozinkina, I., Vieli, B.,
1182 Vogel, G.: The COSMO Priority Project “COLOBOC”: Final Technical Report No 27, (No
1183 27), 2015.

1184 Beven, K.: Robert E. Horton’s perceptual model of infiltration processes, *Hydrol. Process.*,
1185 18(17), 3447–3460, doi:10.1002/hyp.5740, 2004.

1186 Bhaskar, A. S., Welty, C., Maxwell, R. M., and Miller, A. J.: Untangling the effects of urban
1187 development on subsurface storage in Baltimore, *Water Resour. Res.*, 51(2), 1158–1181,
1188 doi:10.1002/2014WR016039, 2015.

1189 Bixio, A. C., Gambolati, A. G., Paniconi, A. C., Putti, A. M., Shestopalov, A. V. M., Bublías, V.
1190 N., Bohuslavsky, A. A. S., Kasteltseva, A. N. B., and Rudenko, Y. F.: Modeling
1191 groundwater-surface water interactions including effects of morphogenetic depressions in
1192 the Chernobyl exclusion zone, *Environ. Geol.*, 42(162–177), doi:10.1007/s00254-001-0486-
1193 7, 2002.

1194 Briggs, W. L., Henson, V. E., and McCormick, S. F.: *A Multigrid Tutorial, Second Edition*,
1195 2000.

1196 Brookfield, A. E., Sudicky, E. A., Park, Y. J., and Conant, B.: Thermal transport modelling in a
1197 fully integrated surface/subsurface framework, *Hydrol. Process.*, 23(15), 2150–2164,
1198 doi:10.1002/hyp.7282, 2009.

1199 Brown, P. N., and Saad, Y.: *Hybrid Krylov Methods for Nonlinear Systems of Equations*, SIAM
1200 *J. Sci. Stat. Comput.*, 11(3), 450–481, doi:10.1137/0911026, 1990.

1201 Burstedde, C., Fonseca, J. A., and Kollet, S.: Enhancing speed and scalability of the ParFlow
1202 simulation code, *Comput. Geosci.*, 22(1), 347–361, doi:10.1007/s10596-017-9696-2, 2018.

1203 Camporese, M., Paniconi, C., Putti, M., and Orlandini, S.: Surface-subsurface flow modeling
1204 with path-based runoff routing, boundary condition-based coupling, and assimilation of
1205 multisource observation data, *Water Resour. Res.*, 46(2), doi:10.1029/2008WR007536,
1206 2010.

1207 Castronova, A. M., Goodall, J. L., and Ercan, M. B.: Integrated Modeling within a Hydrologic
1208 Information System: An OpenMI Based Approach, *Environ. Model. Softw.*,
1209 doi:10.1016/j.envsoft, 2013.

1210 Celia, M. A., Bouloutas, E. T., and Zarba, R. L.: A general mass-conservative numerical
1211 solution for the unsaturated flow equation, *Water Resour. Res.*, 26(7), 1483–1496,
1212 doi:10.1029/WR026i007p01483, 1990.

1213 Chow, F. K., Kollet, S. J., Maxwell, R. M., and Duan, Q.: Effects of Soil Moisture Heterogeneity
1214 on Boundary Layer Flow with Coupled Groundwater, Land-Surface, and Mesoscale
1215 Atmospheric Modeling, 17th Symp. Bound. Layers Turbul., doi:10.1016/j.phrs.2010.10.003,
1216 2006.

1217 Collier, A. M., Hindmarsh, A. C., Serban, R., and Woodward, C. S.: User Documentation for
1218 kinsol v2.8.2 (SUNDIALS v2.6.2), , 1, 120, 2015.

- 1219 Condon, L. E., and Maxwell, R. M.: Implementation of a linear optimization water allocation
 1220 algorithm into a fully integrated physical hydrology model, *Adv. Water Resour.*, 60, 135–
 1221 147, doi:10.1016/j.advwatres.2013.07.012, 2013.
- 1222 Condon, L. E., and Maxwell, R. M.: Groundwater-fed irrigation impacts spatially distributed
 1223 temporal scaling behavior of the natural system: a spatio-temporal framework for
 1224 understanding water management impacts, *Environ. Res. Lett.*, 9(3), 034009,
 1225 doi:10.1088/1748-9326/9/3/034009, 2014.
- 1226 Condon, L. E., and Maxwell, R.M.: Evaluating the relationship between topography and
 1227 groundwater using outputs from a continental-scale integrated hydrology model, *Water*
 1228 *Resour. Res.*, 51(8), 6602–6621, doi:10.1002/2014WR016774, 2015.
- 1229 Condon, L. E., Maxwell, R. M., and Gangopadhyay, S.: The impact of subsurface
 1230 conceptualization on land energy fluxes, *Adv. Water Resour.*, 60, 188–203,
 1231 doi:10.1016/J.ADVWATRES.2013.08.001, 2013.
- 1232 Condon, L. E., Hering, A. S., and Maxwell, R. M.: Quantitative assessment of groundwater
 1233 controls across major US river basins using a multi-model regression algorithm, *Adv. Water*
 1234 *Resour.*, 82, 106–123, doi:10.1016/J.ADVWATRES.2015.04.008, 2015.
- 1235 Dai, Y. et al.: The Common Land Model, *Bull. Am. Meteorol. Soc.*, 84(8), 1013–1023,
 1236 doi:10.1175/BAMS-84-8-1013, 2003.
- 1237 Dembo, R. S., and Eisenstat, S. C.: Inexact newton methods, in *SIAM J. Numer. Anal.*, vol. 19,
 1238 pp. 400–408, 1982.
- 1239 Dennis Jr, John E., and R. B. S.: *Numerical Methods for Unconstrained Optimization and*
 1240 *Nonlinear Equations*, 1996.
- 1241 Duniec, G., and Mazur, A.: COLOBOC - MOSAIC parameterization in COSMO model v. 4.8,
 1242 (11), 69–81, 2011.
- 1243 Durbin, P.: An Approach to Local Refinement of Structured Grids An Approach to Local
 1244 Refinement of Structured Grids, *J. Comput. Phys.*, 181, 639–653,
 1245 doi:10.1006/jcph.2002.7147, 2002.
- 1246 Eca, L.: 2D orthogonal grid generation with boundary point distribution control, *J. Comput.*
 1247 *Phys.*, 125(2), 440–453, doi:10.1006/jcph.1996.0106, 1996.
- 1248 Eisenstat, S. C., and Walker, H. F.: Choosing the Forcing Terms in an Inexact Newton Method,
 1249 *SIAM J. Sci. Comput.*, 17(1), 16–32, doi:10.1137/0917003, 1996.
- 1250 Ek, M. B., Mitchell, K. E., Lin, Y., Rogers, E., Grunmann, P., Koren, V., Gayno, G., and
 1251 Tarpley, J. D.: Implementation of Noah land surface model advances in the National
 1252 Centers for Environmental Prediction operational mesoscale Eta model, *J. Geophys. Res.*
 1253 *Atmos.*, 108(D22), doi:10.1029/2002JD003296, 2003.
- 1254 Engdahl, N. B., and Maxwell, R. M.: Quantifying changes in age distributions and the
 1255 hydrologic balance of a high-mountain watershed from climate induced variations in
 1256 recharge, *J. Hydrol.*, 522, 152–162, doi:10.1016/j.jhydrol.2014.12.032, 2015.
- 1257 Engdahl, N. B., McCallum, J. L., and Massoudieh, A.: Transient age distributions in subsurface
 1258 hydrologic systems, *J. Hydrol.*, 543, 88–100, doi:10.1016/J. Hydrol.2016.04.066, 2016.
- 1259 Falgout, R. D., and Yang, U. M.: Hypre: A Library of High Performance Preconditioners, in
 1260 *International Conference on Computational Science.*, 632–641, Springer, Berlin, 2002.
- 1261 Falgout, R. D., Baldwin, C., Bosl, W., Hornung, R., Shumaker, D., Smith, S., Woodward, C. S.,
 1262 and Tompson, A. F. B.: *Enabling Computational Technologies for Subsurface Simulations*,
 1263 1999.
- 1264 Ferguson, I. M., and Maxwell, R. M.: *Groundwater-Land Surface-Atmosphere Feedbacks:*

1265 Impacts of Groundwater Pumping and Irrigation on Land-Atmosphere Interactions, Proc.
1266 xviii Int. Conf. Comput. Methods Water Resour., 722–729, 2010.

1267 Ferguson, I. M., and Maxwell, R. M.: Human impacts on terrestrial hydrology: climate change
1268 versus pumping and irrigation, *Environ. Res. Lett.*, 7(4), 044022, doi:10.1088/1748-
1269 9326/7/4/044022, 2012.

1270 Frei, S., Fleckenstein, J. H., Kollet, S. J., and Maxwell, R. M.: Patterns and dynamics of river-
1271 aquifer exchange with variably-saturated flow using a fully-coupled model, *J. Hydrol.*,
1272 375(3–4), 383–393, doi:10.1016/j.jhydrol.2009.06.038, 2009.

1273 Gasper, F., Goergen, K., Shrestha, P., Sulis, M., Rihani, J., Geimer, M., and Kollet, S. J.:
1274 Implementation and scaling of the fully coupled Terrestrial Systems Modeling Platform
1275 (TerrSysMP v1.0) in a massively parallel supercomputing environment - A case study on
1276 JUQUEEN (IBM Blue Gene/Q), *Geosci. Model Dev.*, 7(5), 2531–2543, doi:10.5194/gmd-
1277 7-2531-2014, 2014.

1278 Gebler, S., Kollet, S., Qu, W., and Vereecken, H.: High resolution modelling of soil moisture
1279 patterns with ParFlow-CLM: Comparison with sensor network data, , 17, 2015, 2015.

1280 Gilbert, J. M., and Maxwell, R. M.: Examining regional groundwater-surface water dynamics
1281 using an integrated hydrologic model of the San Joaquin River basin, *Hydrol. Earth Syst.*
1282 *Sci. Discuss.*, 1–39, doi:10.5194/hess-2016-488, 2016.

1283 Gustafson, J. L.: Reevaluating amdahl’s law, 31(5), 532–533, 1988.

1284 Haussling, H. ., and Coleman, R.: A method for generation of orthogonal and nearly orthogonal
1285 boundary-fitted coordinate systems, *J. Comput. Phys.*, 43(2), 373–381, doi:10.1016/0021-
1286 9991(81)90129-7, 1981.

1287 Hindmarsh, A. C., Brown, P. N., Grant, K. E., Lee, S. L., Serban, R., Shumaker, D. E., and
1288 Woodward, C. S.: SUNDIALS: Suite of nonlinear and differential/algebraic equation
1289 solvers, *ACM Trans. Math. Softw.*, 31(3), 363–396, doi:10.1145/1089014.1089020, 2005.

1290 Ian F. M., Jefferson, J. L., Maxwell, R. M., Kollet, S. J.: Effects of root water uptake formulation
1291 on simulated water and energy budgets at local and basin scales, *Env. Earth Sci.*, 75(316),
1292 doi:DOI 10.1007/s12665-015-5041-z, 2016.

1293 Ivanov, V. Y., Vivoni, E. R., Bras, R. L., and Entekhabi, D.: Catchment hydrologic response
1294 with a fully distributed triangulated irregular network model, *Water Resour. Res.*, 40(11),
1295 1–23, doi:10.1029/2004WR003218, 2014.

1296 Jefferson, J. L., and Maxwell, R. M.: Evaluation of simple to complex parameterizations of bare
1297 ground evaporation, *J. Adv. Model. Earth Syst.*, 7, 1075–1092, doi:10.1002/
1298 2014MS000398. Received, 2015.

1299 Jefferson, J. L., Gilbert, J. M., Constantine, P. G., and Maxwell, R.M.: Active subspaces for
1300 sensitivity analysis and dimension reduction of an integrated hydrologic model, *Comput.*
1301 *Geosci.*, 83, 127–138, doi:10.1016/j.cageo.2015.07.001, 2015.

1302 Jefferson, J. L., Maxwell, R. M., and Constantine, P. G.: Exploring the Sensitivity of
1303 Photosynthesis and Stomatal Resistance Parameters in a Land Surface Model, *J.*
1304 *Hydrometeorol.*, 18(3), 897–915, doi:10.1175/JHM-D-16-0053.1, 2017.

1305 Jiang, X., Niu, G. Y., and Yang, Z. L.: Impacts of vegetation and groundwater dynamics on
1306 warm season precipitation over the Central United States, *J. Geophys. Res. Atmos.*, 114(6),
1307 1–15, doi:10.1029/2008JD010756, 2009.

1308 Jones, J. E., and Woodward, C. S.: Preconditioning Newton- Krylov Methods for Variably
1309 Saturated Flow, in 13th International Conference on Computational Methods in Water
1310 Resources, Calgary, Alberta, Canada, 2000.

- 1311 Jones, J. E., and Woodward, C. S.: Newton-Krylov-multigrid solvers for large-scale, highly
 1312 heterogeneous, variably saturated flow problems, *Adv. Water Resour.*, 24(7), 763–774,
 1313 doi:10.1016/S0309-1708(00)00075-0, 2001.
- 1314 Keune, J., Gasper, F., Goergen, K., Hense, A., Shrestha, P., Sulis, M., and Kollet, S.: Studying
 1315 the influence of groundwater representations on land surface-atmosphere feedbacks during
 1316 the European heat wave in 2003, *J. Geophys. Res.*, 121(22), 13,301–13,325,
 1317 doi:10.1002/2016JD025426, 2016.
- 1318 Khorsandi, E., Kollet, S., Venema, V., and Simmer, C.: Investigating the effect of bottom
 1319 boundary condition placement on ground heat storage in climate time scale simulations
 1320 using ParflowE, *Geophys. Res.*, 16(4), 2014, doi:10.1029/2006GL028546, 2014.
- 1321 Kirkner, D. J., and Reeves, H.: Multicomponent Mass Transport With Homogeneous and
 1322 Heterogeneous Chemical Reactions' Effect of the Chemistry on the Choice of Numerical
 1323 Algorithm 1. Theory, *Water Resour. Res.*, 24(10), 1719–1729, 1988.
- 1324 Koch, J., Cornelissen, T., Fang, Z., Bogena, H., Diekkrüger, B., Kollet, S., and Stisen, S.: Inter-
 1325 comparison of three distributed hydrological models with respect to seasonal variability of
 1326 soil moisture patterns at a small forested catchment, *J. Hydrol.*, 533, 234–249,
 1327 doi:10.1016/j.jhydrol.2015.12.002, 2016.
- 1328
- 1329 Kollet, S., Sulis, M., Maxwell, R. M., Paniconi, C., Putti, M., Bertoldi, G., Coon, E. T., Cordano,
 1330 E., Endrizzi, S., Kikinon, E., Mouche, E., Mugler, C., Young-Jin Park, J. C. Refsgaard,
 1331 Stisen Simo, and E. S.: The integrated hydrologic model intercomparison project, IH-MIP2:
 1332 A second set of benchmark results to diagnose integrated hydrology and feedbacks, *Water*
 1333 *Resour. Res.*, 52(1), 1–20, doi:10.1002/2014WR015716, 2017.
- 1334 Kollet, S. J.: Influence of soil heterogeneity on evapotranspiration under shallow water table
 1335 conditions: transient, stochastic simulations, *Environ. Res. Lett.*, 4, 035007,
 1336 doi:10.1088/1748-9326/4/3/035007, 2009.
- 1337 Kollet, S. J.: Optimality and inference in hydrology from entropy production considerations:
 1338 synthetic hillslope numerical experiments., *Hydrol. Earth Syst. Sci.*, 12, 5123–5149, 2015.
- 1339 Kollet, S. J., and Maxwell, R. M.: Integrated surface-groundwater flow modeling: A free-surface
 1340 overland flow boundary condition in a parallel groundwater flow model, *Adv. Water*
 1341 *Resour.*, 29(7), 945–958, doi:10.1016/j.advwatres.2005.08.006, 2006.
- 1342 Kollet, S. J., and Maxwell, R. M.: Capturing the influence of groundwater dynamics on land
 1343 surface processes using an integrated, distributed watershed model, *Water Resour. Res.*,
 1344 44(2), 1–18, doi:10.1029/2007WR006004, 2008a.
- 1345 Kollet, S. J., and Maxwell, R. M.: Demonstrating fractal scaling of baseflow residence time
 1346 distributions using a fully-coupled groundwater and land surface model, *Geophys. Res.*
 1347 *Lett.*, 35(7), 1–6, doi:10.1029/2008GL033215, 2008b.
- 1348 Kollet, S. J., Cvijanovic, I., Schüttemeyer, D., Maxwell, R. M., Moene, A. F., and Bayer, P.: The
 1349 Influence of Rain Sensible Heat and Subsurface Energy Transport on the Energy Balance at
 1350 the Land Surface, *Vadose Zo. J.*, 8(4), 846, doi:10.2136/vzj2009.0005, 2009.
- 1351 Kollet, S. J., Maxwell, R. M., Woodward, C. S., Smith, S., Vanderborcht, J., Vereecken, H., and
 1352 Simmer, C.: Proof of concept of regional scale hydrologic simulations at hydrologic
 1353 resolution utilizing massively parallel computer resources, *Water Resour. Res.*, 46(4), 1–7,
 1354 doi:10.1029/2009WR008730, 2010.
- 1355 Kumar, M., Duffy, C. J., and Salvage, K. M.: A second-order accurate, finite volume-based,
 1356 integrated hydrologic modeling (FIHM) framework for simulation of surface and subsurface

1357 flow, *Vadose Zo. J.*, 8(4), 873, doi:10.2136/vzj2009.0014, 2009.

1358 LaBolle, E. M., Ahmed, A. A., and Fogg, G. E.: Review of the Integrated Groundwater and
1359 Surface-Water Model (IGSM), *Ground Water*, 41(2), 238–246, doi:10.1111/j.1745-
1360 6584.2003.tb02587.x, 2003.

1361 Levis, S., and Jaeger, E. B.: COSMO-CLM2 : a new version of the COSMO- CLM model
1362 coupled to the Community Land Model coupled to the Community Land Model, *Clim.*
1363 *Dyn.*, 37(November), 1889–1907, doi:10.1007/s00382-011-1019-z, 2011.

1364 Li, [L., Steefel, C. I., Kowalsky, M. B., Englert, A., and Hubbard, S. S. et al.](#): Effects of physical
1365 and geochemical heterogeneities on mineral transformation and biomass accumulation
1366 during uranium bioremediation at Rifle, Colorado, *J. Contam. Hydrol.*, 11, 45–63, 2010.

1367 Li, L., Steefel, C. I., and Yang, L.: Scale dependence of mineral dissolution rates within single
1368 pores and fractures, *Geochim. Cosmochim. Acta*, 72, 360–377,
1369 doi:10.1016/j.gca.2007.10.027, 2007.

1370 Markstrom, S. L., Niswonger, R. G., Regan, R. S., Prudic, D. E., and Barlow, P. M.:
1371 GSFLOW—Coupled Ground-Water and Surface-Water Flow Model Based on the
1372 Integration of the Precipitation-Runoff Modeling System (PRMS) and the Modular Ground-
1373 Water Flow Model (MODFLOW-2005), U.S. Geol. Surv., (Techniques and Methods 6-D1),
1374 240, 2008.

1375 Maxwell, R. M., and Miller, N. L.: Development of a Coupled Land Surface and Groundwater
1376 Model, *J. Hydrometeorol.*, 6, 233–247, doi:10.1175/JHM422.1, 2005.

1377 Maxwell, R. M.: Infiltration in Arid Environments: Spatial Patterns between Subsurface
1378 Heterogeneity and Water-Energy Balances, *Vadose Zo. J.*, 9(4), 970,
1379 doi:10.2136/vzj2010.0014, 2010.

1380 Maxwell, R. M.: A terrain-following grid transform and preconditioner for parallel, large-scale,
1381 integrated hydrologic modeling, *Adv. Water Resour.*, 53, 109–117,
1382 doi:10.1016/j.advwatres.2012.10.001, 2013.

1383 Maxwell, R. M., Welty, C., and Tompson, A. F. B.: Streamline-based simulation of virus
1384 transport resulting from long term artificial recharge in a heterogeneous aquifer, *Adv. Water*
1385 *Resour.*, 26(10), 1075–1096, doi:10.1016/S0309-1708(03)00074-5, 2003.

1386 Maxwell, R. M., Chow, F. K., and Kollet, S. J.: The groundwater–land-surface–atmosphere
1387 connection: Soil moisture effects on the atmospheric boundary layer in fully-coupled
1388 simulations, *Adv. Water Resour.*, 30(12), 2447–2466, doi:10.1016/j.advwatres.2007.05.018,
1389 2007.

1390 Maxwell, R. M., Lundquist, J. K., Mirocha, J. D., Smith, S. G., Woodward, C. S., and Tompson,
1391 A. F. B.: Development of a Coupled Groundwater–Atmosphere Model, *Mon. Weather Rev.*,
1392 139(1), 96–116, doi:10.1175/2010MWR3392.1, 2011.

1393 Maxwell, R. M., Condon, L. E., and Kollet, S. J.: A high-resolution simulation of groundwater
1394 and surface water over most of the continental US with the integrated hydrologic model
1395 ParFlow v3, *Geosci. Model Dev*, 923–937, doi:10.5194/gmd-8-923-2015, 2015.

1396 [Maxwell, R. M. et al.: Surface-subsurface model intercomparison: A first set of benchmark](#)
1397 [results to diagnose integrated hydrology and feedbacks, *Water Resour. Res.*, 50, 1531–](#)
1398 [1549, doi:10.1002/2013WR013725, 2014.](#)

1399

1400 Maxwell, R. M. et al.: ParFlow User ’s Manual, 2016.

1401 Meehl, G. A., Covey, C., McAvaney, B., Latif, M., and Stouffer, R. J.: Overview of the coupled
1402 model intercomparison project, *Bull. Am. Meteorol. Soc.*, 86(1), 89–93,

1403 doi:10.1175/BAMS-86-1-89, 2005.

1404 Meyerhoff, S. B., and Maxwell, R. M.: Using an integrated surface-subsurface model to simulate
1405 runoff from heterogeneous hillslopes, in xviii International Conference on Water Resources,
1406 CIMNE, Barcelona, 2010.

1407 Michalakes, J., Dudhia, J., Gill, D., Klemp, J., and Skamarock, W.: Design of a next-generation
1408 regional weather research and forecast model, Towar. Teracomputing, 19999.

1409 Michalakes, J., Chen, S., Dudhia, J., Hart, L., Klemp, J., Middlecoff, J., and Skamarock, W.:
1410 Development of a next-generation regional weather research and forecast model, Towar.
1411 Teracomputing, 2001.

1412 Mikkelsen, K. M., Maxwell, R. M., Ferguson, I., Stednick, J. D., Mccray, J. E., and Sharp, J. O.:
1413 Mountain pine beetle infestation impacts: Modeling water and energy budgets at the hill-
1414 slope scale, *Ecohydrology*, 6(1), 64–72, doi:10.1002/eco.278, 2013.

1415 Mironov, D., Heise, E., Kourzeneva, E. and Ritter, B.: Implementation of the lake
1416 parameterisation scheme FLake into the numerical weather prediction model COSMO,
1417 *Boreal Environ. Res.*, 6095(April), 218–230, 2010.

1418 Mobley, C. D., and Stewart, R. S.: On the numerical generation of boundary-fitted orthogonal
1419 curvilinear coordinate systems, *J. Comput. Phys.*, 34(1), 124–135, doi:10.1016/0021-
1420 9991(80)90117-5, 1980.

1421 Molders, N., and Ruhaak, W.: On the impact of explicitly predicted runoff on the simulated
1422 atmospheric response to small-scale land-use changes—an integrated modeling approach,
1423 *Atmos. Res.*, 63, 2002.

1424 Navarre-Sitchler, A., Steefel, C. I., Sak, P. B., and Brantley, S. L.: A reactive-transport model for
1425 weathering rind formation on basalt, *Geochim. Cosmochim. Acta*, 75, 7644–7667,
1426 doi:10.1016/j.gca.2011.09.033, 2011.

1427 Oleson, K. W. et al.: Improvements to the Community Land Model and their impact on the
1428 hydrological cycle, *J. Geophys. Res. Biogeosciences*, 113(G1), doi:10.1029/2007JG000563,
1429 2008.

1430 Osei-Kuffuor, D., Maxwell, R. M., and Woodward, C. S.: Improved numerical solvers for
1431 implicit coupling of subsurface and overland flow, *Adv. Water Resour.*, 74,
1432 doi:10.1016/j.advwatres.2014.09.006, 2014.

1433 Panday, S., and Huyakorn, P. S.: A fully coupled physically-based spatially-distributed model for
1434 evaluating surface/subsurface flow, *Adv. Water Resour.*, 27(4), 361–382,
1435 doi:10.1016/j.advwatres.2004.02.016, 2004.

1436 Rahman, M., Sulis, M., and Kollet, S. J.: Evaluating the dual-boundary forcing concept in
1437 subsurface-land surface interactions of the hydrological cycle, *Hydrol. Process.*, 30(10),
1438 1563–1573, doi:10.1002/hyp.10702, 2016.

1439 Ren, D., and Xue, M.: A revised force–restore model for land surface modeling, *Am. Meteorol.*
1440 *Soc.*, 2004.

1441 Reyes, B., Maxwell, R. M., and Hogue, T. S.: Impact of lateral flow and spatial scaling on the
1442 simulation of semi-arid urban land surfaces in an integrated hydrologic and land surface
1443 model, *Hydrol. Process.*, 30(8), 1192–1207, doi:10.1002/hyp.10683, 2016.

1444 Richards, L. A.: Capillary conduction of liquids through porous mediums, *J. Appl. Phys.*, 1(5),
1445 318–333, doi:10.1063/1.1745010, 1931.

1446 Rigon, R., Bertoldi, G., and Over, T. M.: GEOtop: A Distributed Hydrological Model with
1447 Coupled Water and Energy Budgets, *J. Hydrometeorol.*, 7(3), 371–388,
1448 doi:10.1175/jhm497.1, 2006.

1449 Rihani, J.F., Chow, F. K., Fotini K., and Maxwell, R. M.: Isolating effects of terrain and soil
1450 moisture heterogeneity on the atmospheric boundary layer: Idealized simulations to
1451 diagnose land-atmosphere feedbacks, *J. Adv. Model. Earth Syst.*, 6, 513–526,
1452 doi:10.1002/2014MS000371. Received, 2015.

1453 Rihani, J. F., Maxwell, M. R., and Chow, F. K.: Coupling groundwater and land surface
1454 processes: Idealized simulations to identify effects of terrain and subsurface heterogeneity
1455 on land surface energy fluxes, *Water Resour. Res.*, 46(12), 1–14,
1456 doi:10.1029/2010WR009111, 2010.

1457 Ryskin, G., and Leal, L.: Orthogonal mapping, *J. Comput. Phys.*, 50(1), 71–100,
1458 doi:10.1016/0021-9991(83)90042-6, 1983.

1459 Saad, Y., and Schultz, M. H.: GMRES: A Generalized Minimal Residual Algorithm for Solving
1460 Nonsymmetric Linear Systems, *SIAM J. Sci. Stat. Comput.*, 7(3), 856–869,
1461 doi:10.1137/0907058, 1986.

1462 Seck, A., Welty, C., and Maxwell, R. M.: Spin-up behavior and effects of initial conditions for
1463 an integrated hydrologic model Alimatou, *Water Resour. Res.*, 51, 2188–2210,
1464 doi:10.1002/2014WR016371. Received, 2015.

1465 Seuffert, G., Gross, P., Simmer, A. C., and Wood, E. F.: The Influence of Hydrologic Modeling
1466 on the Predicted Local Weather: Two-Way Coupling of a Mesoscale Weather Prediction
1467 Model and a Land Surface Hydrologic Model, *J. Hydrometeorol.*, 3, 2002.

1468 Shen, C., and Phanikumar, M. S.: A process-based, distributed hydrologic model based on a
1469 large-scale method for surface-subsurface coupling, *Adv. Water Resour.*, 33(12), 1524–
1470 1541, doi:10.1016/j.advwatres.2010.09.002, 2010.

1471 Shi, Y., Davis, K. J., Zhang, F., and Duffy, C. J.: Evaluation of the Parameter Sensitivities of a
1472 Coupled Land Surface Hydrologic Model at a Critical Zone Observatory, *J.*
1473 *Hydrometeorol.*, 15(1), 279–299, doi:10.1175/JHM-D-12-0177.1, 2014.

1474 Shrestha, P., Sulis, M., Masbou, M., Kollet, S., and Simmer, C.: A Scale-Consistent Terrestrial
1475 Systems Modeling Platform Based on COSMO, CLM, and ParFlow, *Mon. Weather Rev.*,
1476 142, doi:10.1175/MWR-D-14-00029.1, 2014.

1477 Shrestha, P., Sulis, M., Simmer, C., and Kollet, S.: Impacts of grid resolution on surface energy
1478 fluxes simulated with an integrated surface-groundwater flow model, *Hydrol. Earth Syst.*
1479 *Sci*, 19, 4317–4326, doi:10.5194/hess-19-4317-2015, 2015.

1480 Simmer, C. et al.: Monitoring and modeling the terrestrial system from pores to catchments: The
1481 transregional collaborative research center on patterns in the soil-vegetation-atmosphere
1482 system, *Bull. Am. Meteorol. Soc.*, 96(10), 1765–1787, doi:10.1175/BAMS-D-13-00134.1,
1483 2015.

1484 Skamarock, W. C., and Klemp, J. B.: A Time-Split Nonhydrostatic Atmospheric Model
1485 for Weather Research and Forecasting Applications, , (001), 1–43, 2007.

1486 Skamarock, W. C., Klemp, J. B., Dudhia, J., Gill, D. O., Barker, D. M., Wang, W., and Powers,
1487 J. G.: A description of the advanced research WRF Version 2, 2005.

1488 Smith, S. G., Ashby, S. F., Falgout, R. D., and Tomsom, A. F. B.: The parallel performance of a
1489 groundwater flow code on the CRAY T3D. In *Proceedings of the Seventh SIAM*
1490 *Conference on Parallel Processing for Scientific Computing*, 131, 1995.

1491 Srivastava, V., Graham, W., Muñoz-Carpena, R., and Maxwell, R. M.: Insights on geologic and
1492 vegetative controls over hydrologic behavior of a large complex basin – Global Sensitivity
1493 Analysis of an integrated parallel hydrologic model, *J. Hydrol.*, 519, 2238–2257,
1494 doi:10.1016/J. Hydrol.2014.10.020, 2014.

1495 Steefel, C. I., and Yabusaki, S. B.: OS3D/GIMRT software for modeling multicomponent-
1496 multidimensional reactive transport, Richland, WA, 1996.

1497 Steefel, C. I.: CrunchFlow Software for Modeling Multicomponent Reactive Flow and Transport
1498 User's Manual, 2009.

1499 Steefel, C. I., and Van Cappellen, P.: A new kinetic approach to modeling water-rock interaction:
1500 The role of nucleation, precursors, and Ostwald ripening, *Geochim. Cosmochim. Acta*,
1501 54(10), 2657–2677, doi:10.1016/0016-7037(90)90003-4, 1990.

1502 Steefel, C. I., and Lasaga, A. C.: A coupled model for transport of multiple chemical species and
1503 kinetic precipitation/dissolution reactions with application to reactive flow in single phase
1504 hydrothermal systems, *Am. J. Sci.*, 294(5), 529–592, doi:10.2475/ajs.294.5.529, 1994.

1505 Steefel, C. I. et al.: Reactive transport codes for subsurface environmental simulation, *Comput.*
1506 *Geosci.*, 19(3), 445–478, doi:10.1007/s10596-014-9443-x, 2015.

1507 Steiner, A. L., Pal, J. S., Giorgi, F., Dickinson, R. E., and Chameides, W. L.: The coupling of the
1508 Common Land Model (CLM0) to a regional climate model (RegCM), *Theor. Appl.*
1509 *Climatol.*, 82(3–4), 225–243, doi:10.1007/s00704-005-0132-5, 2005.

1510 Steiner, A. L., Pal, J. S., Rauscher, S. A., Bell, J. L., Diffenbaugh, N. S., Boone, A., Sloan, L. C.,
1511 and Giorgi, F.: Land surface coupling in regional climate simulations of the West African
1512 monsoon, *Clim. Dyn.*, 33(6), 869–892, doi:10.1007/s00382-009-0543-6, 2009.

1513 Sudicky, E. A., Jones, J. P., Park, Y. J., Brookfield, A. E., and Colautti, D.: Simulating complex
1514 flow and transport dynamics in an integrated surface-subsurface modeling framework,
1515 *Geosci. J.*, 12(2), 107–122, doi:10.1007/s12303-008-0013-x, 2008.

1516 Sulis, M., Meyerhoff, S. B., Paniconi, C., Maxwell, R. M., Putti, M., and Kollet, S. J.: A
1517 comparison of two physics-based numerical models for simulating surface water-
1518 groundwater interactions, *Adv. Water Resour.*, 33(4), 456–467,
1519 doi:10.1016/j.advwatres.2010.01.010, 2010.

1520 Sulis, M., Williams, J. L., Shrestha, P., Diederich, M., Simmer, C., Kollet, S. J., and Maxwell,
1521 R. M.: Coupling Groundwater, Vegetation, and Atmospheric Processes: A Comparison of
1522 Two Integrated Models, *J. Hydrometeorol.*, 18(5), 1489–1511, doi:10.1175/JHM-D-16-
1523 0159.1, 2017.

1524 Therrien, R and Sudicky, E.: Three-dimensional analysis of variably-saturated flow and solute
1525 transport in discretely- fractured porous media, *J. Contam. Hydrol.*, 23(95), 1–44,
1526 doi:10.1016/0169-7722(95)00088-7, 1996.

1527 Tompson, A. F. B., Ababou, R., and Gelhar, L. W.: Implementation of the three-dimensional
1528 turning bands random field generator, *Water Resour. Res.*, 25(10), 2227–2243,
1529 doi:10.1029/WR025i010p02227, 1989.

1530 Tompson, A. F. B., Ashby, S. F., and Falgout, R. D.: Use of high performance computing to
1531 examine the effectiveness of aquifer remediation, 1994.

1532 Tompson, A. F. B., Falgout, R. D., Smith, S. G., Bosl, W. J., and Ashby, S. F.: Analysis of
1533 subsurface contaminant migration and remediation using high performance computing,
1534 *Adv. Water Resour.*, 22(3), 203–221, doi:10.1016/S0309-1708(98)00013-X, 1998.

1535 Tompson, A. F. B., Carle, S. F., Rosenberg, N. D., and Maxwell, R. M.: Analysis of
1536 groundwater migration from artificial recharge in a large urban aquifer: A simulation
1537 perspective, *Water Resour. Res.*, 35(10), 2981–2998, doi:10.1029/1999WR900175, 1999.

1538 Valcke, S.: The OASIS3 coupler : a European climate modelling community software, *Geosci.*
1539 *Model Dev*, 6, 373–388, doi:10.5194/gmd-6-373-2013, 2013.

1540 Valcke, S., Balaji, V., Bentley, P., Guilyardi, E., Lawrence, B., and Pascoe, C.: Developing a

1541 Common Information Model for climate models and data, *Geophys. Res. Abstr.*, 11, 10592,
1542 2009.

1543 Valcke, S., Balaji, V., Craig, A., Deluca, C., Dunlap, R., Ford, R. W., Jacob, R., Larson, J., and
1544 Kuinghttons, O. R.: Model Development Coupling technologies for Earth System
1545 Modelling, *Geosci. Model Dev.*, 5, 1589–1596, doi:10.5194/gmd-5-1589-2012, 2012.

1546 VanderKwaak, J. E.: Numerical simulation of flow and chemical transport in integrated surface-
1547 subsurface hydrologic systems, 1999.

1548 VanGenuchten, M. T.: A Closed-form Equation for Predicting the Hydraulic Conductivity of
1549 Unsaturated Soils, *Soil Sci. Soc. Am. J.*, 44, 892–898,
1550 doi:10.2136/sssaj1980.03615995004400050002x, 1980.

1551 Visbal, M., and Knight, D.: Generation of orthogonal and nearly orthogonal coordinates with
1552 gridcontrol near boundaries, *AIAA J.*, 20(3), 305–306, doi:10.2514/3.7915, 1982.

1553 Vogel, B., Vogel, H., Bangert, M., Lundgren, K., Rinke, R., and Stanelle, T.: The comprehensive
1554 model system COSMO-ART – Radiative impact of aerosol on the state of the atmosphere
1555 on the regional scale, *Atmos. Chem. Phys.*, 9, 8661–8680, 2009.

1556 Volker, J.: Multigrid Methods, , doi:10.1137/1.9781611971057, 1987.

1557 Wagner, S., Fersch, B., Yuan, Y., Yu, Z., and Kunstmann, H.: Fully coupled atmospheric-
1558 hydrological modeling at regional and long-term scales: Development, application, and
1559 analysis of WRF-HMS, *Water Resour. Res.*, 52(4), 3187–3211,
1560 doi:10.1002/2015WR018185, 2016.

1561 Weill, S., Mouche, E., and Patin, J.: A generalized Richards equation for surface/subsurface flow
1562 modelling, *J. Hydrol.*, 366(1–4), 9–20, doi:10.1016/j.jhydrol.2008.12.007, 2009.

1563 Weill, S., Mazzia, A., Putti, M., and Paniconi, C.: Coupling water flow and solute transport into
1564 a physically-based surface-subsurface hydrological model, *Adv. Water Resour.*, 34(1), 128–
1565 136, doi:10.1016/j.advwatres.2010.10.001, 2011.

1566 Williams, J. L., and Maxwell, R. M.: Propagating Subsurface Uncertainty to the Atmosphere
1567 Using Fully Coupled Stochastic Simulations, *J. Hydrometeorol.*, 12(1994), 690–701,
1568 doi:10.1175/2011JHM1363.1, 2011.

1569 Williams, J. L., Maxwell, R. M., and Monache, L. D.: Development and verification of a new
1570 wind speed forecasting system using an ensemble Kalman filter data assimilation technique
1571 in a fully coupled hydrologic and atmospheric model, *J. Adv. Model. Earth Syst.*, 5(4), 785–
1572 800, doi:10.1002/jame.20051, 2013.

1573 Wood, B. D.: The role of scaling laws in upscaling, *Adv. Water Resour.*, 32(5), 723–736,
1574 doi:10.1016/j.advwatres.2008.08.015, 2009.

1575 Woodward, S. C.: A Newton-Krylov-multigrid solver for variably saturated flow problems,
1576 Proceedings on the Twelfth International Conference on Computational Methods in Water
1577 Resources, in *Computational Mechanics Publications*, vol. 2, pp. 609–616, 1998.

1578 Xu, L., Raman, S., and Madala, R. V.: A review of non-hydrostatic numerical models for the
1579 atmosphere, *Math. Subj. Classif*, 1991.

1580 Xue, M., Droegemeier, K. K., and Wong, V.: The Advanced Regional Prediction System
1581 (ARPS) - A multi-scale nonhydrostatic atmospheric simulation and prediction tool. Part II:
1582 Model dynamics and verification, *Meteorol. Atmos. Phys.*, 75, 161–193,
1583 doi:10.1007/s007030170027, 2000.

1584 Zhufeng F., Bogena, H., Kollet, S., Koch, J. H. V.: Spatio-temporal validation of long-term 3D
1585 hydrological simulations of a forested catchment using empirical orthogonal functions and
1586 wavelet coherence analysis, *Hydrology*, 529(1754–1767), 2015.

